Naval Surface Warfare Center

Carderock Division

West Bethesda, MD 20817-5700

NSWCCD-80-TR-2016/003 **January 2016**

Naval Architecture and Engineering Department

Technical Report

A GUIDE FOR MEASURING, ANALYZING, AND EVALUATING ACCELERATIONS RECORDED DURING SEAKEEPING TRIALS OF HIGH-SPEED CRAFT

by

Michael R. Riley, The Columbia Group
Kelly D. Haupt, NSWCCD
Dr. Timothy W. Coats, NSWCCD
Dr. H.C. Neil Ganey, NSWCCD
Heidi P. Murphy, NSWCCD

REPORT DOCUMENTATION PAGE

Form Approved
OMB No. 0704-0188

1. REPORT DATE	**2. REPORT TYPE**	**3. DATES COVERED** *(From - To)*
20-09-2015	Final	Jul 2015 to Sep 2015

4. TITLE AND SUBTITLE
A Guide for Measuring, Analyzing, and Evaluating Accelerations Recorded During Seakeeping Trials of High-Speed Craft

5a. CONTRACT NUMBER

5b. GRANT NUMBER

5c. PROGRAM ELEMENT NUMBER

6. AUTHOR(S)
Michael R. Riley (TCG), Kelly D. Haupt, Dr. Timothy W. Coats, Dr. H.C. Neil Ganey, Heidi P. Murphy

5d. PROJECT NUMBER

5e. TASK NUMBER

5f. WORK UNIT NUMBER

7. PERFORMING ORGANIZATION NAME(S) AND ADDRESS(ES)
NAVSEA Carderock
Naval Surface Warfare Center
Carderock Division (Code 83)
9500 Macarthur Boulevard
West Bethesda, MD 20817-5700

8. PERFORMING ORGANIZATION REPORT NUMBER
NSWCCD-80-TR-2016/003

9. SPONSORING / MONITORING AGENCY NAME(S) AND ADDRESS(ES)
NAVSEA Carderock
Naval Surface Warfare Center
Carderock Division
9500 MacArthur Blvd
West Bethesda, MD 20817-5700

10. SPONSOR/MONITOR'S ACRONYM(S)

11. SPONSOR/MONITOR'S REPORT NUMBER(S)

12. DISTRIBUTION / AVAILABILITY STATEMENT
DISTRIBUTION STATEMENT A. Approved for public release; distribution is unlimited.

13. SUPPLEMENTARY NOTES

14. ABSTRACT
This report is a guide for measuring and analyzing acceleration data recorded during trials of full-scale high speed craft. Minimum requirements for instrumentation systems are summarized, and standardized data processing methods are presented to foster commonality and comparability between different organizations. Examples of recorded data are shown to illustrate data processing and data analysis methods. Numerous approaches to comparing and evaluating data sets are summarized.

15. SUBJECT TERMS
Wave impact planing craft acceleration data analysis

16. SECURITY CLASSIFICATION OF:			**17. LIMITATION OF ABSTRACT**	**18. NUMBER OF PAGES**	**19a. NAME OF RESPONSIBLE PERSON**
					Dr. Timothy Coats
a. REPORT	**b. ABSTRACT**	**c. THIS PAGE**			**19b. TELEPHONE NUMBER**
Unclassified	Unclassified	Unclassified	See 12.	56	757-462-4161

Standard Form 298 (Rev. 8-98)
Prescribed by ANSI Std. Z39.18

THIS PAGE INTENTIONALLY LEFT BLANK

CONTENTS

FIGURES

TABLES

SYMBOLS, ABBREVIATIONS, AND ACRONYMS

π ..... ratio of circle circumference to its diameter
θ ..... impact angle of deck relative to horizon
A/D..... Analogue-to-digital
A_{MAX} ..... maximum or peak acceleration
A_W ..... frequency weighted (i.e., band-pass filtered) acceleration
A(t)..... acceleration time history
ASCII..... American Standards Code for Information Interchange
ASRS ..... acceleration shock response spectrum
CCD ..... Combatant Craft Division
dB..... decibel
dc..... direct current
DRI..... dynamic response index
DSRS ..... relative displacement shock response spectrum
FFT..... Fast Fourier Transform
g ..... acceleration due to gravity (32.2 ft/sec^2, 9.81 m/sec^2)
Hz..... Hertz (cycles per second)
IC ..... impact count
ICI ..... impact count index
IMU..... inertial measurement unit
ISO ..... International Standards Organization
LCG ..... longitudinal center of gravity
m ..... meter
M..... integer value of 3, 10, or 100
MEMS..... micro electro-mechanical system
MPa..... megapascals
N..... number of wave impacts with peak amplitude greater than RMS acceleration
RIB..... rigid inflatable boat

RMS ..... root mean square
RSI ..... ride severity index
RSP ..... ride severity profile
s/s ..... samples per second
S_{ed} ..... daily equivalent static compression dose
t ..... time
T ..... wave impact shock pulse duration
T_L ..... length of acceleration record
V ..... vertical change in craft rigid body velocity
VDV ..... vibration dose value
W_K ..... band pass filter (i.e., frequency weighting function)
x ..... surge axis positive forward
y ..... sway axis positive to port
z ..... surge axis positive up

ADMINISTRATIVE INFORMATION

This report was prepared by the Combatant Craft Division (CCD, Code 83) of the Naval Architecture and Engineering Department at the Naval Surface Warfare Center, Carderock Division (NSWCCD) with funding provided by Naval Surface Warfare Center, Carderock Division under the Naval Innovative Science and Engineering (NISE) Section 219 research and development program.

ACKNOWLEDGEMENTS

The authors would like to thank Dr. Jack L. Price, Director of Research, Naval Surface Warfare Center, Carderock Division for overall management of wave slam phenomenology investigations. Mr. Jason Bautista, NSWCCD, Combatant Craft Division (CCD), Test and Evaluation Branch, Code 835, developed software for computing vibration dose values. Mr. Dean M. Schleicher, Technical Warrant Holder for Combatant Craft and Boats, Naval Sea Systems Command, Mr. David Pogorzelski, CCD Test and Evaluation Branch Head, and Mr. Kenneth Davis, CCD Deputy Director completed in-depth reviews and provided numerous comments that improved the report. Their combined expertise and contributions in combatant craft design, acquisition, systems integration, and seakeeping trials data acquisition are sincerely appreciated.

SUMMARY

This report is a guide for measuring and analyzing acceleration data recorded during trials of full-scale high speed craft. Minimum requirements for instrumentation systems are summarized, and standardized data processing methods are presented to foster commonality and comparability between different organizations. Examples of recorded data are shown to illustrate data processing and data analysis methods. Numerous approaches to comparing and evaluating data sets are summarized. While the primary focus is on recorded accelerations, the data acquisition, processing, and comparison methods are also applicable to measured pitch, roll, and yaw motions.

INTRODUCTION

Background

Long before the development of motion measurement systems experienced seamen could evaluate the handling and ride in a ship or small craft with their sensory perceptions of heave, surge, sway, pitch, roll, and yaw, as well as the linear and rotational rates of change of the motions. It is a complex environment that combines rigid body motions in six degrees of freedom driven by forces from random wave encounters. But subjective evaluations even by experienced operators did not satisfy the need of naval architects and marine engineers for numbers to guide performance evaluations or develop hull designs. Accelerometers were the first sensors developed to measure craft motions [1, 2][1], and the advent of computers and digital data processing led directly to the use of statistical approaches to characterize random seaways [3, 4]. It was known early on however, that in addition to statistical methods, a deterministic method would be useful for characterizing individual wave impacts and the conditions just prior to impact [5].

Statistical methods provide knowledge about motion variations in a large data set collected over time. Deterministic methods provide knowledge about the physical cause and effects relationship between the load caused by one wave input and the resulting response motion at a point on the craft [6]. When combined the two approaches provide lessons learned for addressing a broader range of design and comparative analysis topics than obtained from just one approach. This report summarizes both statistical and deterministic methods for analyzing and evaluating accelerations in high-speed planing craft.

[1] Numbers in brackets are references listed at the end of the guide.

Terminology

Acceleration signal. The acceleration signal is the stream of data being transmitted by an accelerometer that is recorded during a test. In some standards the word signal is used synonymously with record or time history.

Acceleration record. The acceleration record is the stream of data that has been recorded.

Acceleration time history. The acceleration time history is a plot of the acceleration record as a function of time. It is a visual display of the signal that was recorded.

Crest Factor. The crest factor is the modulus of the maximum peak acceleration of a band-pass filtered acceleration time history to its root-mean-square (RMS) acceleration. The band-pass filter is described in ISO-2631 Part 1 [7].

Modal decomposition. Modal decomposition is the mathematical separation of an observed experimental response into its different relevant modes of response (e.g., rigid body motions and vibrations).

Modal superposition. The linear addition of relevant modes of structural response that yields the final observed response is referred to as modal superposition.

Rigid body motion. Rigid body motions of a craft are its absolute translations (heave, surge, and sway) and rotations (pitch, roll, and yaw) in a seaway.

Shock. The term shock is used to imply mechanical shock, as opposed to electrical shock or chemical shock. Mechanical shock is an excitation of a physical system that is characterized by suddenness and severity. Shock-input is often used synonymously with severe wave impact, wave slam, or impulsive load.

Impact Velocity. Impact velocity is the rigid body velocity of a craft (at a measure point) at the time of wave impact. It is equal to (but opposite in sign) the change in rigid body velocity caused by a wave impact.

Vertical direction. Vertical means normal to a flat deck. In a Cartesian coordinate system used in this guide the vertical direction (heave) is labeled Z, motion forward (surge) is the X direction, motion to port (sway) is the positive Y direction. Deck mounted accelerometers installed in full-scale trials are typically oriented so that the vertical direction of the gage is oriented normal to the deck. As shown in Figure 1, the vertical direction of the accelerometer may therefore be oriented at some angle (theta) relative to the horizon during impacts.

Vibration. Vibrations are flexural motions of structural elements at or adjacent to installed accelerometers. They are typically transient vibrations excited by wave impacts as well as sustained vibrations excited by operating machinery.

Wave slam. A wave slam is a violent impact between a craft and an incident wave. A wave impact is typically considered a more general term that may imply both low severity and high severity wave encounters.

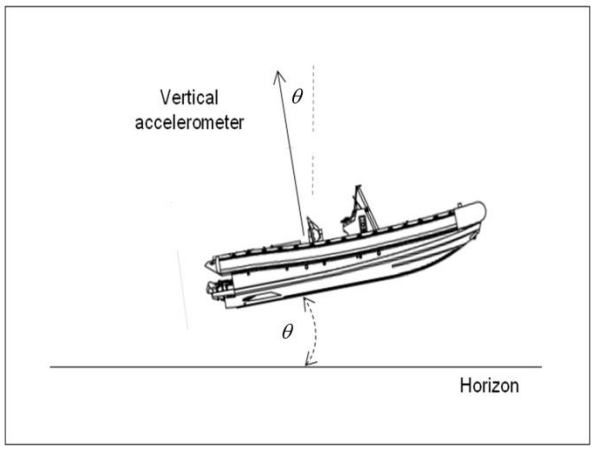

Figure 1. Orientation of Vertical Accelerometer

MEASURING ACCELERATIONS

The presumption that motions data has been acquired properly cannot be overstated, because improperly collected data will result in meaningless analysis results. Attention must be paid to measurement system powering, sensor mounting, signal conditioning, and data recording. [8 - 12]. Appropriate anti-aliasing filtering must also be applied as part of the analog-to-digital (A/D) conversion process. The following paragraphs provide a general overview of instrumentation systems for measuring accelerations in high-speed craft. Another reference on the subject is "Behind the Scenes of Peak Acceleration Measurement" [13].

Digital data acquisition requires the signal to be band limited to preclude aliased frequency components in the data signal. Testing experience has shown that sufficient information for evaluating seakeeping motions of high-speed craft can be achieved with a data bandwidth of dc (direct current) to 100 hertz (Hz). Higher bandwidths for studying craft system vibrations are beyond the scope of this guide.

Data Acquisition System

Modern digital data acquisition and measurement systems are self-contained (i.e., they do not need an external computer), relatively inexpensive, highly reliable, and available from a number of sources. Nearly all equipment has a minimum of 16-bit A/D conversion with consequent signal resolution of 65,536 parts (98 decibel (dB) signal/noise), and many manufacturers offer 24-bit A/D systems. A data acquisition system should have a minimum of 16-bit A/D, and provisions for assuring alias signal rejection through fixed low-pass hardware pre-filters, oversampling, or a combination of both. A resolution of better than 0.001 g is achievable for a 25 g accelerometer coupled with a 16-bit data acquisition system.

The minimum sampling rate for acquisition of high-speed craft data should be 512 samples per second (s/s). Most data acquisition systems are capable of sample rates per channel in the range of 100,000 samples per second or greater. Sampling at 512 s/s or greater is easily achievable.

A pre-filter should be employed in the hardware prior to A/D conversion to prevent alias frequencies in the data. A 100-Hz low-pass filter with characteristics similar to a 4-pole Butterworth filter is suggested.

Data may be stored in a binary form as a matter of efficiency, but is should be converted to a human-readable ASCII (American Standard Code for Information Interchange) format. Data saved in ASCII format can be easily reviewed using text editor software like Microsoft®'s Notepad and Wordpad, or can be opened using spreadsheet software like Microsoft®'s Excel. Likewise, ASCII data can be analyzed using engineering software like DADiSP®, MATLAB®, or LabVIEW™, for example.

Accelerometers

Piezoresistive, servo, or micro electro-mechanical system (MEMS) type accelerometers should be used because they have dc response (i.e., the ability to operate over a frequency range beginning at zero Hz) that can measure -1 g during the free-fall phase. They should have a minimum frequency response of dc to 1,000 Hz, a nominal full-scale range of ± 25 g, and a nominal sensitivity of 50 mV/g or greater. Perhaps the most popular, economical, and widely available are MEMS accelerometers, with prices in the range of a few hundreds of dollars each. Piezoelectric accelerometers should not be used because they have a lower frequency limit greater than zero Hz. They do not measure craft freefall after wave encounters at high speeds.

Accelerometer Location

Rigid body linear and rotation measurements in the six degrees of freedom typically provide the primary data for evaluating and comparing seakeeping characteristics of different craft. This is achieved with accelerometers that measure surge, sway, and heave at any cross-section of a craft, and an inertial measurement unit (IMU) for measuring rigid body pitch, roll, and yaw about the craft's longitudinal center of gravity (LCG). These gages should be installed on structure that is relatively rigid. A relatively rigid location is one that will minimize recorded vibrations. This includes positions on massive structure or on decks above or next to vertical supports like stiffeners and bulkheads.

Other measurements on more flexible craft structure may be just as important depending upon the trial objectives. For example, there may be specific objectives requiring that sensors be positioned at less rigid locations to measure shock inputs to electronics equipment, to measure deck plate response frequencies, or to evaluate engine mount vibration characteristics.

ANALYZING RECORDED ACCELERATIONS

Zero Axis Shift

Plots of raw unprocessed acceleration data recorded during at-sea trials may appear to oscillate about a non-zero axis (referred to as a DC bias in the signal). This is due to the inability to "zero the gage" while underway, even in very calm sea conditions. The shift may be imperceptibly small or as large as plus or minus 1 g or more. The first step in data processing is therefore to shift the data axis in a process called demeaning or shifting the acceleration zero axis. It is a computational process where the average of all digitized data points in a record is computed, and then the average is subtracted from each data point. Some standards recommend the use of a high-pass filter to remove DC bias from an acceleration record. This is not recommended for wave impact studies where the effect of gravity on vertical accelerations is important. In some cases the accelerometer can be zeroed before the trials, so demeaning will not be required, for example, when the craft is ashore on its trailer.

Fourier Spectrum Analysis

Accelerometers are very sensitive instruments. They measure the acceleration of motions attributed to the six rigid body modes, motions due to global flexure like hull girder bending (i.e., whipping) if present, and motions of structural vibrations at the gage location caused by wave impacts and by machinery systems [14]. But structural vibrations are not the primary interest in rough-water seakeeping trials, so accelerometers are typically positioned at relatively stiff or massive locations, such as on deck plating directly over stiffeners or bulkheads to minimize the vibration content. But even when accelerometers are located on relatively hard spots, they are sensitive enough to record accelerations of the millimeter vibrations of plating in the vicinity of the accelerometer. Unfortunately the accelerations associated with vibrations may not be small during wave impacts. They can be equal to or greater than rigid body heave accelerations caused by the vertical force of a wave impact at a cross-section of a craft. It is therefore important to know how much of the signal is vibration motion compared to other motion content.

An algorithm called a Fast Fourier Transform (FFT) can be used to evaluate the frequency content in an acceleration time history [15]. It generates a plot called a Fourier spectrum (also referred to as an FFT plot) that plots the relative amplitudes of the sinusoidal components (that can be superimposed to create the time history) as a function of the component frequency. It is useful for identifying vibration frequency content in an acceleration record. The example Fourier spectrum in Figure 2 indicates the dominant rigid body motions due to the wave impacts are less than 2 Hz. Humps or peaks in the spectrum at approximately 25 Hz, 40 Hz, and 55 Hz are due to different modes of structural vibration in the signal. Separating an unfiltered acceleration record into its different modes of response is referred to as response mode decomposition.

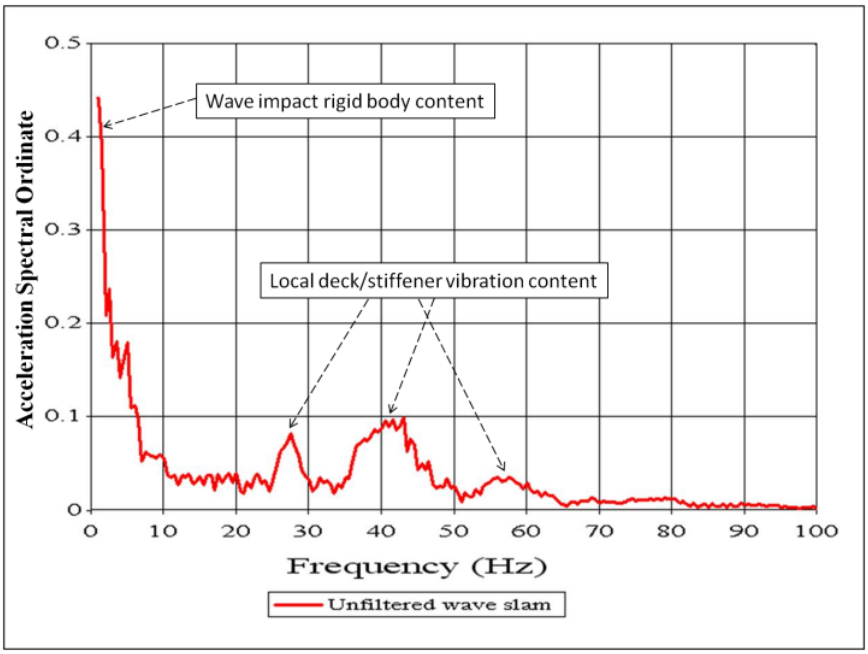

Figure 2. Fourier Spectrum of Vertical Acceleration Record[2]

Low-pass Filter

The low-pass filter passes the frequency content of the majority of a signal's frequencies below the filter cutoff frequency. For example, a 20-Hz 4-pole Butterworth low-pass filter passes the frequency content from dc to just below the cutoff frequency (i.e., 20 Hz). At 20 Hz the signal amplitude is reduced by a factor of $1/\sqrt{2}$ (approximately equal to a 3 dB reduction in signal strength) and higher frequencies are attenuated at a rate of 24 dB per octave [8]. The Fourier spectrum in Figure 2 indicates that use of a 10-Hz low-pass filter would effectively remove the vibration content from 25 Hz to 60 Hz.

Low-pass filtering is basically a reverse engineering modal decomposition process used to extract the rigid body content from an acceleration record [17]. Rigid body heave accelerations are used as a measure of wave impact load in units of "g" in the vertical direction. Figure 3 shows several wave impacts where the unfiltered acceleration is the gray curve and the rigid body motion content is the black curve. The shape (including the rate of acceleration application), peak amplitude, and duration of the wave impact "spike" are key parameters when studying the effects of wave impacts on hull structure, equipment, and people [18].

Low-pass filtering may not be appropriate for all investigations that analyze craft acceleration data. For example, in the study of the effects of different engine vibration mounts the high-frequency vibration motions above and below the mounts would be of interest, so low-

[2]All plots shown in the report were created using UERDTools [16].

pass filters would not be appropriate. Appendix C presents example applications where cutoff frequencies greater than 10 Hz were used to evaluate acceleration data.

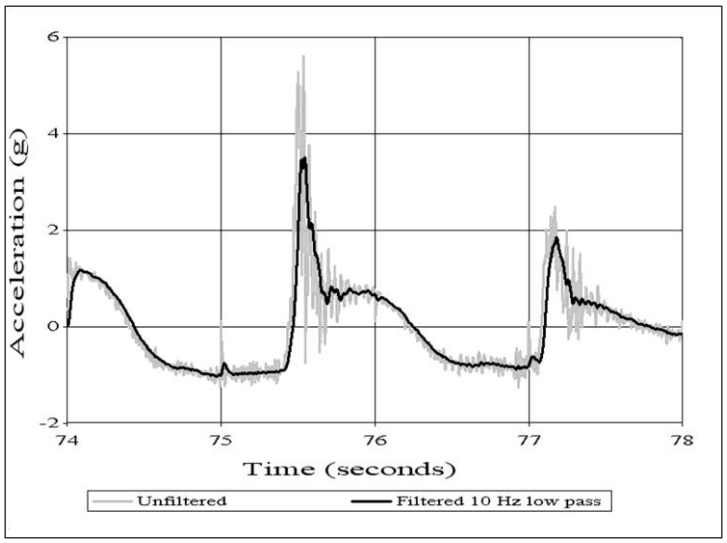

Figure 3. Estimated Rigid Body Acceleration

STATISTICAL ANALYSES

StandardG

StandardG is a software package originally developed by CCD that applies a low-pass filter for estimating rigid body content in the recorded acceleration, a peak counting routine for extracting the rigid body peak accelerations, and an algorithm that computes the average of the highest $1/N^{th}$ peak accelerations used in naval architecture applications [19]. The use of the *StandardG* process enables comparisons of acceleration data results developed by different researchers working at different organizations.

StandardG can be run using MATLAB™ or Octave™ software and it is available free of charge by contacting the Branch Head of the United States Naval Academy Hydrodynamics Laboratory. Contact information is available at www.usna.edu/Hydrodynamics/Contact.php. The information package includes sample raw acceleration data, explanatory text files, computational results, and tutorial papers and reports.

Two low-pass filter options are available in *StandardG*: a Kaiser filter (1% ripple in stop-band, 5% ripple in band-pass, stop-band frequency 20% greater than the specified cutoff frequency, and a 4-pole Butterworth filter (24 dB per octave attenuation, 6 dB per octave per pole). Unpublished comparisons of the two filters showed differences in estimated peak rigid body accelerations on the order of 2 percent or less. Test reports and papers should always document the cut-off frequency and filter type used to process the acceleration data. Figure 4

shows an example unfiltered acceleration time history recorded during a 528-second run for a planing hull craft transiting in head seas. Each spike is caused by a wave impact.

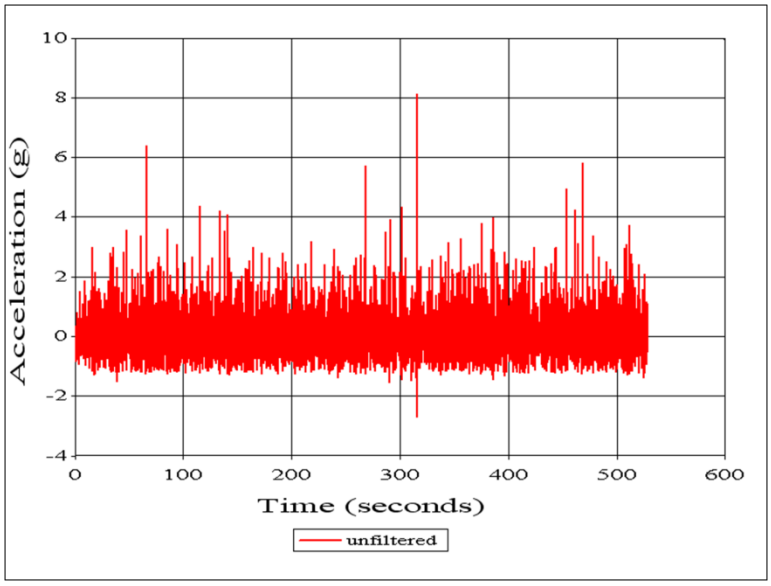

Figure 4. Example Unfiltered Acceleration Record

The plot shown in Figure 5 shows output from the *StandardG* software for the acceleration record shown in Figure 4. The filtered (10 Hz low-pass) peak accelerations for each of the 344 wave impacts larger than the RMS value are plotted largest to smallest. The RMS acceleration is 0.64 g. The largest peak acceleration (labeled in the figure as A_{max}) is 4.63 g, $A_{1/100}$ is 4.19 g, and $A_{1/10}$ is 2.75 g. $A_{1/100}$ is the average of the highest 1 percent of peaks. $A_{1/10}$ is the average of the highest 10 percent of peaks, and $A_{1/3}$ is the average of the highest 33.3 percent of peaks. The RMS acceleration is computed using equation (1). Average of the highest $1/N^{th}$ peak accelerations are computed using equation (2).

$$RMS = \left[\frac{1}{T_L} \int_0^{T_L} A^2(t)\,dt \right]^{\frac{1}{2}} \qquad \text{Equation (1)}$$

$$A_{1/M} = \frac{1}{N/M} \sum_{i=1}^{N/M} A_i \qquad \text{Equation (2)}$$

A(t) is the acceleration time history in units of g, t is time in seconds, T_L is the duration of the acceleration time history in seconds, and A_i are the individual acceleration peaks (extracted from an acceleration time history by *StandardG*) sorted in such a way that the largest amplitude peak acceleration has i =1 and the lowest peak acceleration is i =N. The ratio N/M is a rounded

whole number. N is the number of A_i peak accelerations greater than the RMS value and M is 3, 10, or 100.

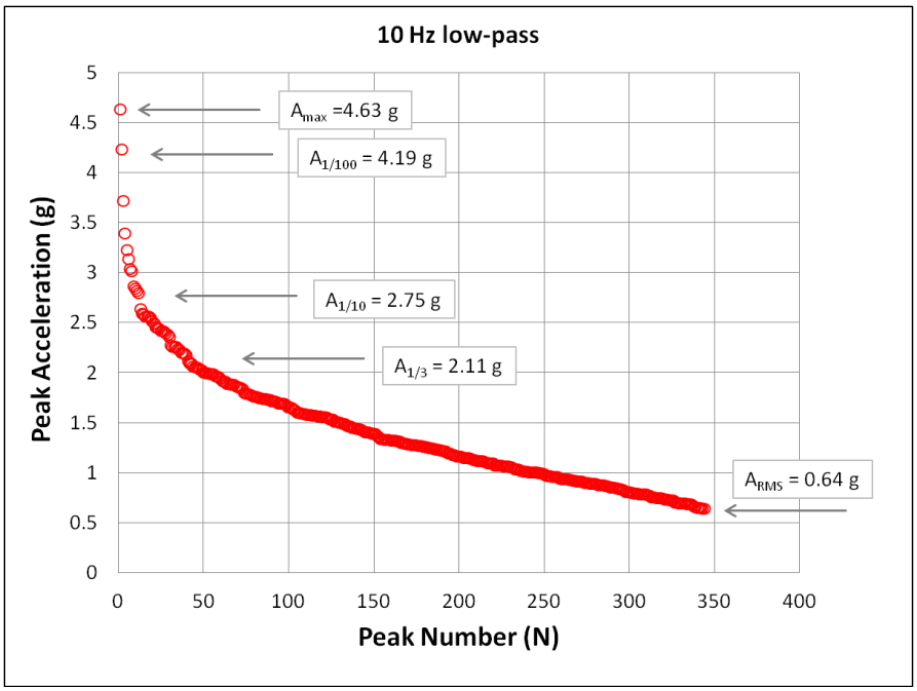

Figure 5. *StandardG* Algorithm Peak Acceleration Output

Comparing Peak Accelerations

The following paragraphs show examples of how all of the A_i peak accelerations computed using *StandardG* can be used to evaluate the severity of a run, or to compare the severity of different runs or different gage locations.

Figure 6 shows the peak accelerations for two different gage locations recorded in the vertical direction on the centerline of an 11-m cabin RIB transiting in head seas at approximately 20 knots when the significant wave height was approximately 4.5 feet (1.37 m) [20]. The recorded data was low-pass filtered at 20 Hz to estimate the peak rigid body accelerations. The 339 circles are the peak accelerations greater than the RMS value for a gage positioned at the LCG. The 359 triangles are for a gage positioned at the forward end of the cabin.

The peak accelerations for the forward cabin are clearly larger (i.e., more severe) than the LCG peaks. The question is "how much larger?" The following sections illustrate different methods for quantifying wave impact severity.

Average $A_{1/N}$ Peak Accelerations

In addition to the RMS value of an acceleration time history, three other statistical acceleration values are used to characterize craft seakeeping characteristics [21, 22]. They are $A_{1/100}$, $A_{1/10}$, and $A_{1/3}$. See equation (2). Table 1 lists average values for the peak accelerations

shown in Figure 6. Plotting formats for comparing these numbers are presented in the Ride Severity Index section later in the report.

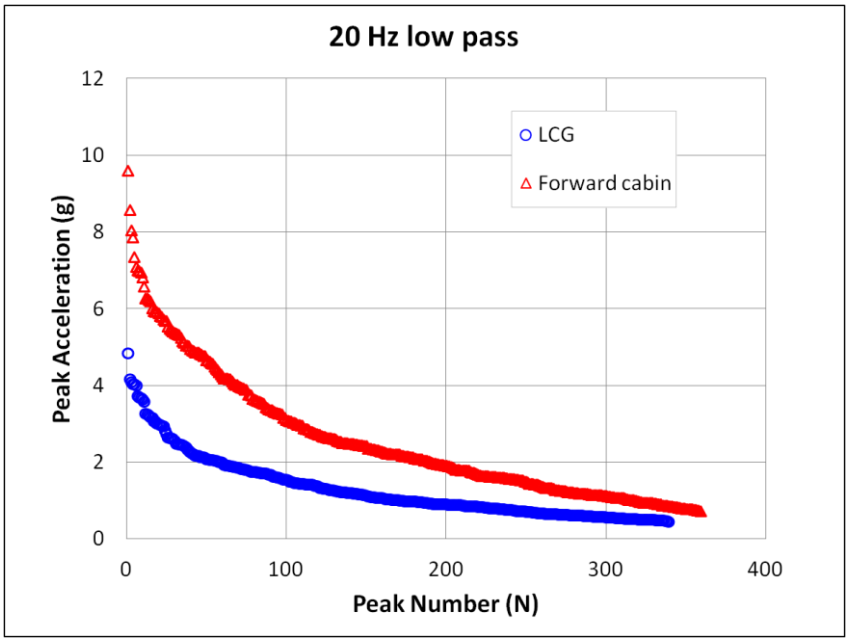

Figure 6. Peak Accelerations for Two Gage Locations

Table 1. Average and RMS Accelerations for Two Gage Locations in Head Seas

Statistic	LCG (g)	Forward Cabin (g)
A 1/100	4.383	8.753
A 1/10	3.241	6.357
A 1/3	2.256	4.641
RMS	0.466	0.741

The polar plot shown in Figure 7 is a useful format for comparing $A_{1/100}$, $A_{1/10}$, and RMS values for runs in different directions.

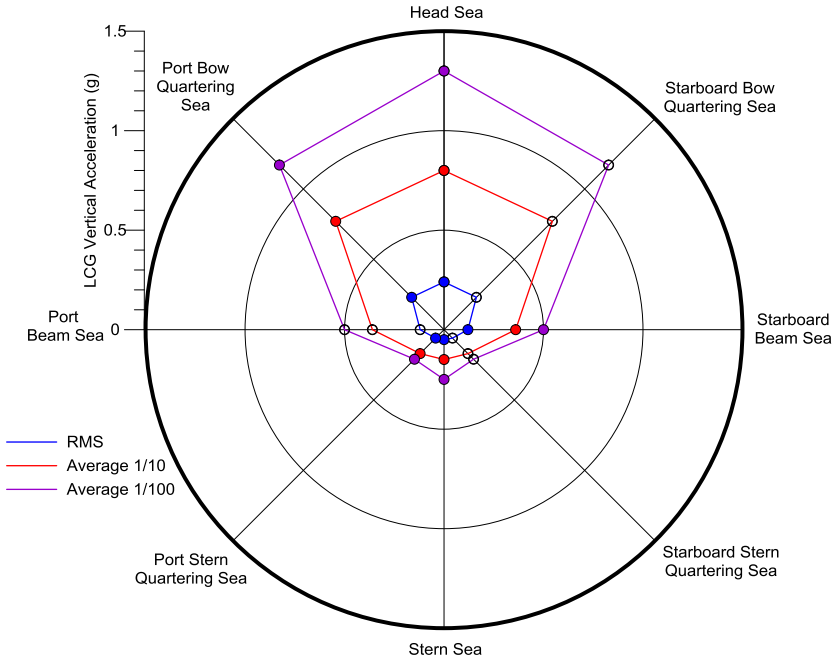

Figure 7. Example Polar Plot for Comparing Different Craft Headings

Impact Count

A histogram format that illustrates the statistical distribution of the peak accelerations computed using *StandardG* is shown in Figure 8. The peak acceleration values from Figure 6 were used to determine how many values fall within predefined intervals (i.e., bins). For example, each data point in Figure 8 is the number of data points in a 0.2 g interval less than or equal to the Peak-G value. The plot shows that for the forward cabin there were 20 peak accelerations less than or equal to 2.6 g (but greater than 2.4 g). For the LCG there were 8 peaks less than or equal to 2.6 g. This histogram has been referred to as the impact count (IC) [23]. It compares the number of peaks at low and high severities. The cumulative distribution plot conveys the same information as a percentage of the total number of peaks.

Impact Count Index

The cumulative distributions for the histograms shown in Figure 8 are shown in Figure 9. It plots the total percentage of peak accelerations less than or equal to the peak acceleration value on the X-axis. It illustrates the higher percentage of peaks occurring at higher values for the forward cabin location (e.g., 80 percent less than or equal to 3.9 g for the forward cabin, 80 percent less than or equal to 1.87 g for the LCG).

The impact count index (ICI) has been used to statistically define the severity of the more severe wave impacts. The 95th percentile and the 99th percentile have been suggested as two levels for describing the severity of an acceleration time history [23]. In the examples shown in Figure 9 the 95th percentile is 5.93 g for the forward cabin and 3.06 g for the LCG. The 99th percentile is 7.40 g for the forward cabin and 4.04 g for the LCG.

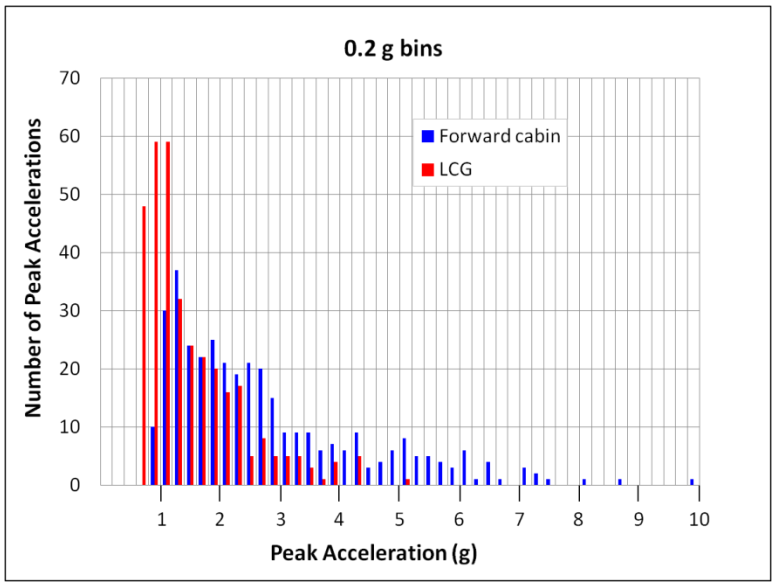

Figure 8. Histogram of 0.2 g Bins

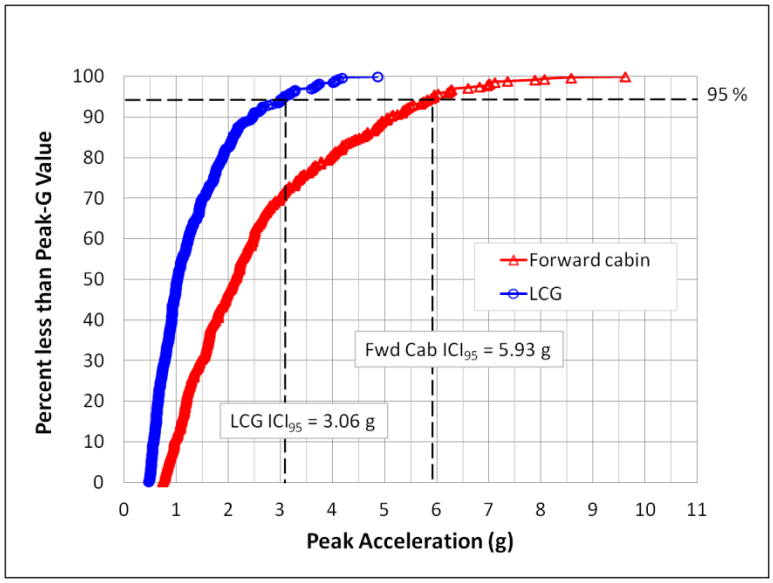

Figure 9. Cumulative Distribution with ICI_{95} Values

Ride Severity Profile

A cumulative distribution curve that plots the percentage of peaks from Figure 6 that are *greater than* or equal to the peak-G level in a semi-log format is shown in Figure 10. The abscissa scale is plotted logarithmically to better illustrate the data points used to compute the $A_{1/100}$, $A_{1/10}$, and $A_{1/3}$ values. For example, the 3 largest data points to the left of 1 percent were used to compute $A_{1/100}$. Likewise the 35 largest values to the left of 10 percent were used to compute $A_{1/10}$, and the 113 largest to the left of 33.33 percent were used to compute $A_{1/3}$.

When the semi-log data plot is color coded with the $A_{1/10}$ values listed in Table 2 the plot is referred to as a Ride Severity Profile (RSP) [24]. The table lists transition zones of $A_{1/10}$ values for evaluating human comfort and performance in high-speed craft. The values evolved as a result of subjective feedback from naval crews, experienced test coxswains, and test engineers and naval architects who participate in high-speed trials. There is no known causal relationship between the $A_{1/10}$ parameter and perceived comfort or the ability to perform mission functions with or without limitations. Its continued use as an interim metric for correlation with craft acceleration data is based on aligning an average acceleration value (e.g., $A_{1/10}$) with averaged descriptions of transition zones (i.e., averaged feedback from different people and operating conditions). In other words, as peak accelerations increase with increasing craft speed or wave steepness, a range of accelerations may correlate better with transition zones than a single parameter like the maximum peak acceleration in a data set. Additional studies should be pursued that systematically investigate parameters and conditions affecting human performance and comfort in a wave impact environment. Figure 11 shows the peak accelerations for the two example gage locations with the crew comfort and performance transition zones.

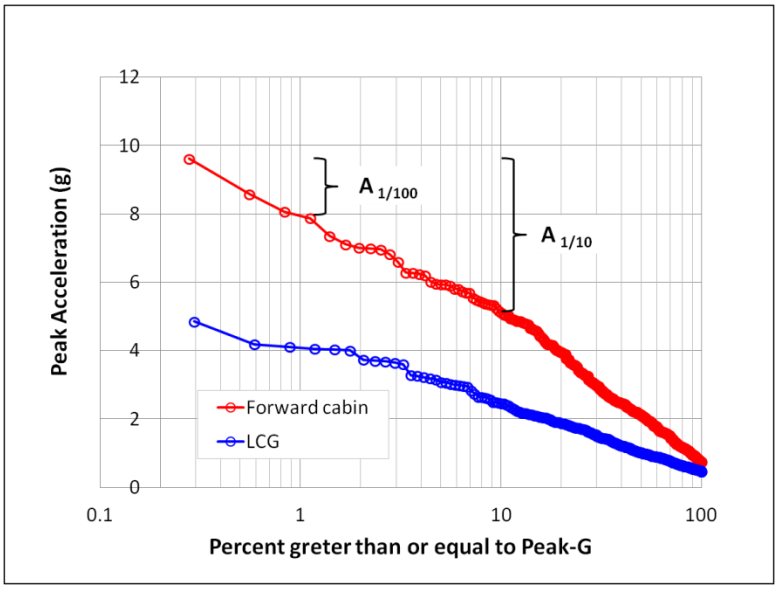

Figure 10. Semi-log peak acceleration data plot

Table 2. Interim $A_{1/10}$ Transition Zones for Crew Comfort and Performance

$A_{1/10}$	Transition Zones
< 1.5 g	Conditions typically result in a comfortable ride with effective performance for 4 hours or more
1.5 g - 2.0 g	Conditions may transition from a comfortable ride to a ride with limited discomfort
2.0 g - 2.7 g	Conditions transition from a comfortable ride to a ride with discomfort and limited performance
2.7 g - 3.2 g	Conditions transition from discomfort to the onset of extreme discomfort
3.2 g - 5.5 g	Conditions transition from extreme discomfort to the onset of concern for personnel safety
5.5 g - 6.0 g	Conditions transition from extreme discomfort and concern into potentially unsafe conditions with increased risk of safety mishaps

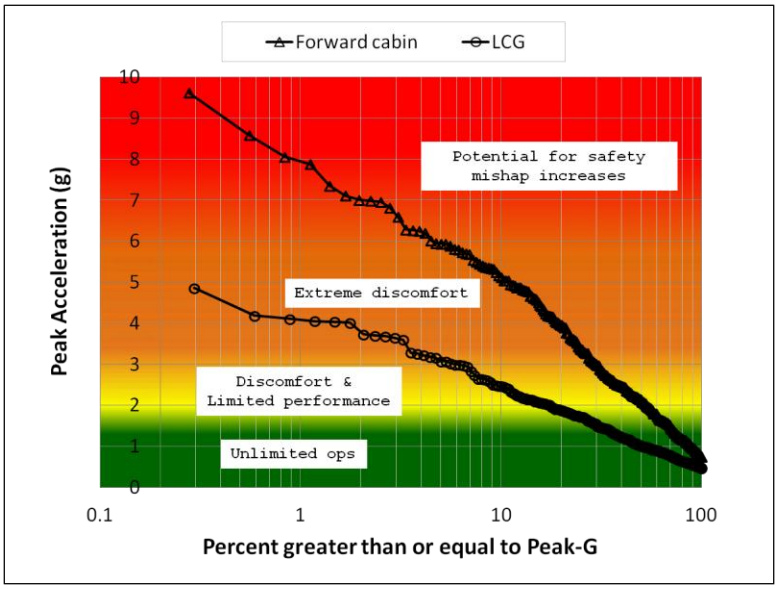

Figure 11. Ride Severity Profile Comparing Two Gage Locations

Ride Severity Index

Figure 12 compares all the LCG peak accelerations (sorted largest to smallest) with all the forward cabin peak accelerations (sorted largest to smallest) from Figure 6. The LCG and forward cabin peaks are plotted as x–y pairs. For example, the largest peak for each is plotted together (x-y pair), then each of the 2nd largest peaks are plotted together, then each of the 3rd largest peaks are plotted together, and so on until all pairs of peak accelerations are plotted. Data

comparison points that fall on the dotted line (slope of one) have equal acceleration values and therefore have the same ride severity. Values below the dotted line indicate a relatively less severe ride compared to the LCG severity and points above the dotted line indicate a more severe ride than the LCG. To construct this plot the peak accelerations for the forward cabin gage less than 0.866 g were deleted to yield the same number of peaks as the LCG gage (i.e., 339 peaks).

The dotted line in Figure 12 with a slope of 2.03 is a linear least square fit of the data with the intercept set equal to zero. The slope is approximately equal to the average ratio of all the peak acceleration pairs, largest to smallest, and can be used as a relative indicator of the ride severity. In this example the forward cabin peak accelerations are on the order of 2.03 (i.e., the slope) times larger than the LCG accelerations.

Figure 13 is a similar comparison but the x – y pairs are the RMS, $A_{1/3}$, $A_{1/10}$, and $A_{1/100}$ values for the LCG and forward cabin gages from Table 1. The ride severity index (RSI) is defined as the slope of the least squares fit line (with zero intercept) of a plot of $A_{1/N}$ and RMS statistics for one condition plotted against $A_{1/N}$ and RMS statistics for another condition [25]. Two conditions have equal ride severity when RSI = 1.0. Values greater than 1.0 correspond to a more severe ride, and values less than 1.0 are less severe. In Figure 13 the ride severity index is 1.99, or the forward cabin location is on the order of 1.99 times more severe than the LCG location. When the average accelerations are used the slopes will be slightly different from the slope when all peak accelerations are used (as in Figure 12).

The ride severity index is a very useful format for comparing different ride severities, including comparisons of different craft, different speeds, different wave heights, different gage locations, and different operational conditions (e.g., with and without ride control).

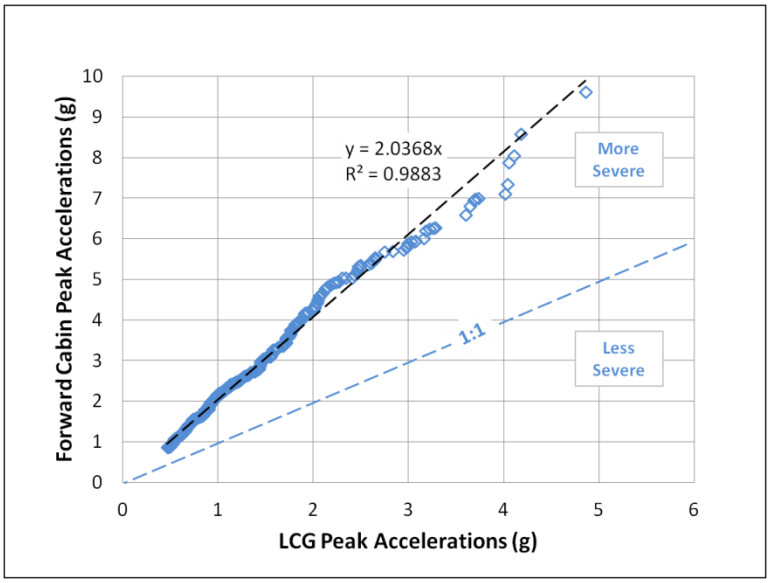

Figure 12. Plot Comparing Two Gage Location Peaks as X – Y Pairs

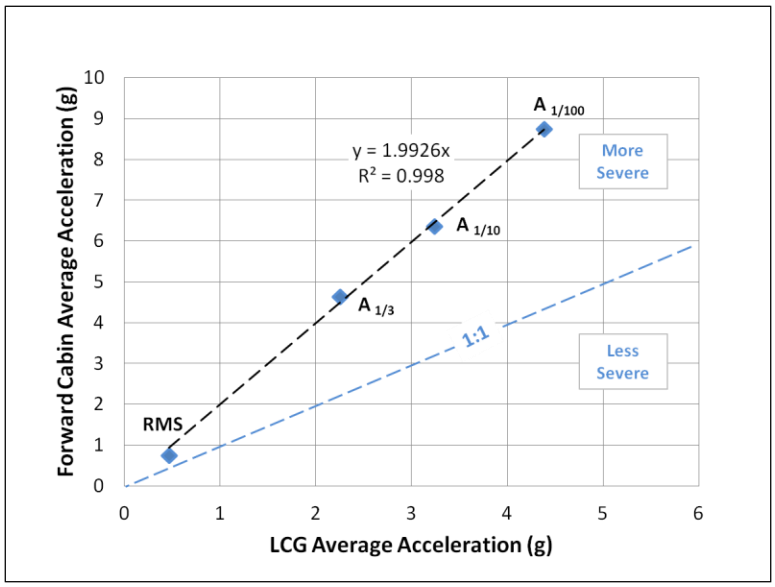

Figure 13. Ride Severity Index Plot for Two Gage Locations

Figure 14 illustrates the comparison of different craft headings, and Figure 15 compares craft with and without a ride control system.

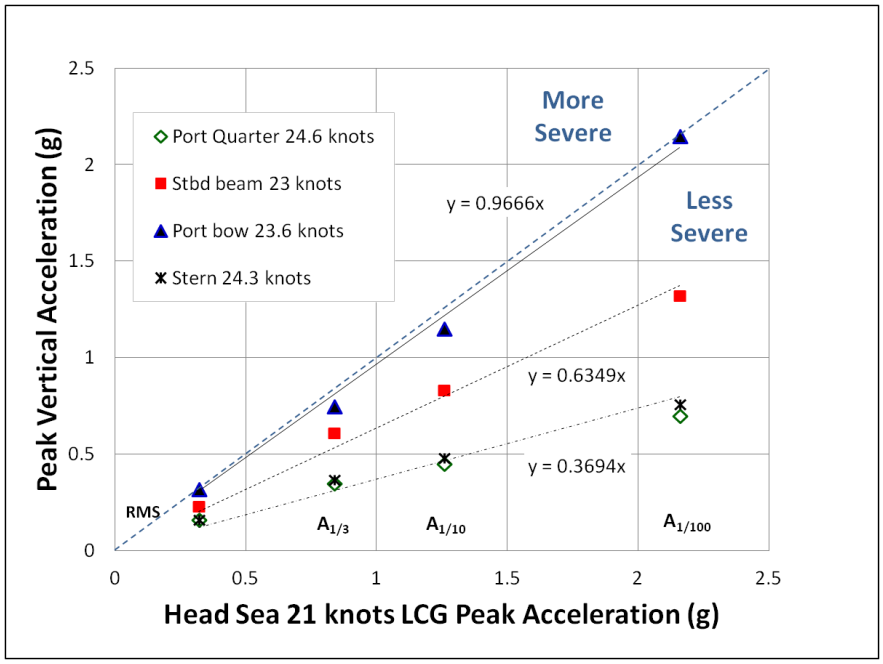

Figure 14. Example Comparison of Different Craft Headings

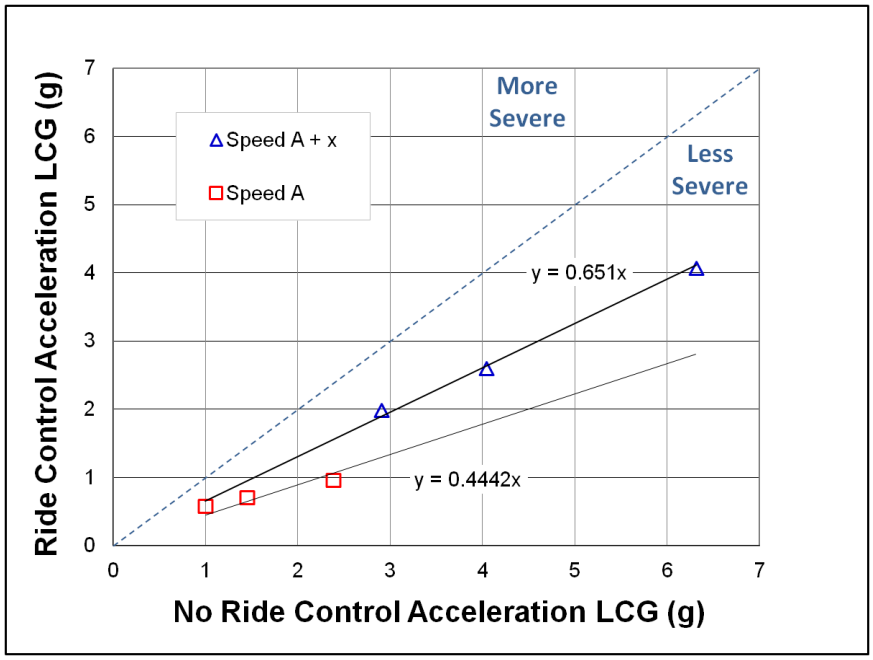

Figure 15. Example Comparison of RSI Values With and Without Ride Control

DETERMINISTIC ANALYSIS APPROACH

Input and Response

Figure 16 shows a typical vertical acceleration response measured at the LCG of a high-speed planing craft. Three separate wave impacts are observed as a very rapid change from a negative acceleration to a positive peak value. The response to each impact is observed to be a combination of rigid body motions and a period of forced vibration. The amplitude of the forced vibration is much larger than the amplitude of the background vibration signal observed prior to each impact. The plot shows that the change in rigid body motion during the wave impact and the duration of the forced vibration response damps out prior to the next impact. This is a very important observation because it means that each impact response is not coupled to the next impact response. Therefore, each wave impact can be analyzed as a single input and response phenomenon [26].

Half-Sine Pulse Approximation

The shape of the rigid body acceleration pulse during a severe wave impact can be simplified for analytical study as a half-sine pulse [27]. Figure 17 illustrates the half-sine representation of the rigid body vertical acceleration pulse for a wave impact where the largest amplitude is A_{max} and the pulse duration is T. The peak acceleration, the duration of the pulse, and the shape of the pulse, including the initial rate of acceleration application (i.e., jerk), are important characteristics when quantifying the severity of the wave impact load transmitted through the craft at the gage location.

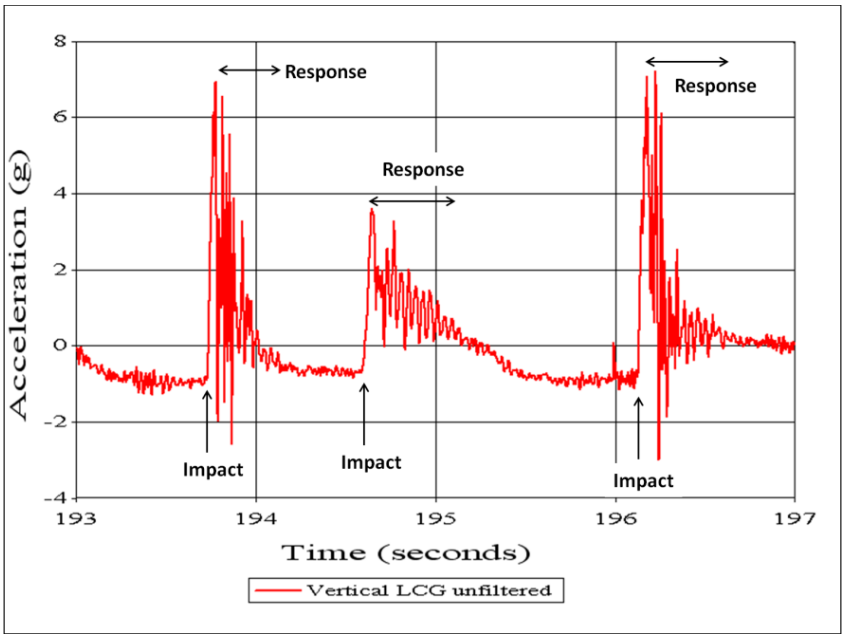

Figure 16. Acceleration Input and Response Phases

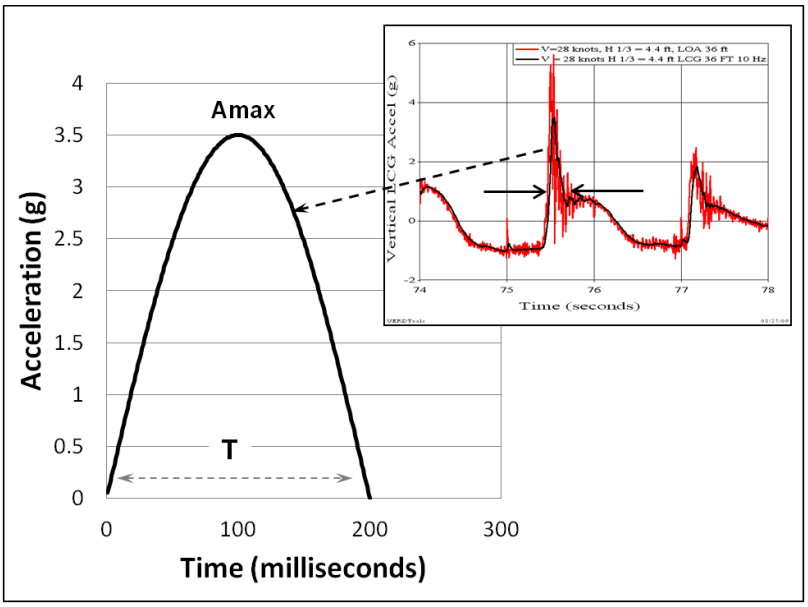

Figure 17. Half-sine Pulse Approximation for a Wave Impact Acceleration Pulse

The area under the acceleration pulse in Figure 17 is the change in velocity caused by the wave impact. It is another important parameter for characterizing the severity of a shock pulse and is useful for planning laboratory drop tests designed to simulate the change in velocity caused by a severe wave impact [28]. It can be shown that the change in velocity for the half-sine pulse is given by equation (3).

$$V = \frac{64.4}{\pi} A_{MAX}\, T \qquad \text{Equation (3)}$$

where V is change in velocity in ft/sec, A_{MAX} is the maximum acceleration in units of g, and T is the pulse duration in seconds.

The impact velocity can also be obtained by direct integration of the acceleration record as shown in Appendix A. The demeaned acceleration record should first be high-pass filtered using a 0.025-Hz high-pass filter before integration to remove residual dc bias. This step reduces velocity drift in the velocity time history. High-pass filter frequencies greater than 0.025 Hz (e.g., 0.1 Hz or higher) are not recommended for planing craft accelerations or laboratory drop tests because they cause the sharp acceleration rise from a negative value to zero to become rounded. This has the effect of incorrectly reducing the calculated impact velocity for severe impacts.

The half-sine pulse approximation has been used for investigating hull design parameters [27], developing laboratory test criteria to ensure equipment is sufficiently rugged to withstand single severe and repeated wave impacts [29], and evaluating the effectiveness of shock isolation seats to mitigate wave impacts [18, 30].

Relative Damage Potential for Single Wave Impacts

A useful yardstick for comparing the relative damage potential of two acceleration pulses (i.e., shock pulses) is the computed maximum compressive relative displacement of a spring (Z_{MAX}) in a single degree of freedom (SDOF) mathematical model. See Appendix B. The maximum compression is proportional to the strain in the spring material, so it is a measure of relative damage potential as strain increases with shock intensity. The shock pulse that creates the largest strain in the spring (i.e., relative displacement) is the more severe pulse. It is a universal tool applicable to any dynamic environment. In the case of high-speed craft wave impacts, the comparison can include the effects of individual wave impacts at different locations on a craft, or different speed or wave height conditions, or the difference between the deck input severity and the severity of the response on a shock isolation seat. The shock inputs (i.e., acceleration time history pulses) can be idealized half-sine pulses or actual time-history acceleration data for individual wave impacts.

TIME DEPENDENT WHOLE BODY VIBRATION DOSES

This section summarizes statistical methods used for estimating the effects of exposure to environments that cause whole-body vibrations and shock responses.

Vibration Dose Value

The vibration dose value (VDV) is a fourth-power vibration dose method used for evaluating human exposure to whole body vibration. It was developed to quantify vibrations with occasional repeated shocks, crest factors larger than 9, or transient vibrations [7]. The crest factor is the ratio of the peak acceleration of the band-pass filtered acceleration time history to its RMS acceleration. The VDV is calculated using equation (4).

$$VDV = \left\{ \int_0^{T_L} \left[A_W(t) \right]^4 dt \right\}^{1/4} \qquad \text{Equation (4)}$$

where T_L is the duration in seconds of the acceleration time history, and A_W is the acceleration time history after it has been band-pass (Wk) filtered in units of m/sec^2.

The Wk band-pass filter (described in ISO 2631-1) reduces the amplitude of frequency components less than 4 Hz and above 8 Hz. In the range 4 Hz to 8 Hz there is no amplitude reduction. The units of VDV are m/sec$^{1.75}$. Figure 18 compares the unfiltered segment of the forward cabin acceleration with 20-Hz low-pass (upper plot) and Wk band-pass filtered accelerations (lower plot).

The Wk band-pass filtered acceleration has peak amplitudes similar to the 20-Hz low-pass filtered acceleration, but the negative portions of the original acceleration record are significantly reduced and the shapes of the acceleration pulses at the time of each wave impact are different. Figure 19 shows how the vibration dose value is a cumulative number that depends upon the duration of the acceleration record. For the forward cabin location the VDV for the 30-second segment is 28.28 m/sec$^{1.75}$. VDV for the 30-second LCG acceleration is 14.61 m/sec$^{1.75}$. For the entire 10-minute trial the VDV for the forward cabin location is 58.04 m/sec$^{1.75}$ and 31.09 m/sec$^{1.75}$ for the LCG. It is recommended that the VDV calculation not be used for single shock events like a laboratory drop test of a shock isolation seat.

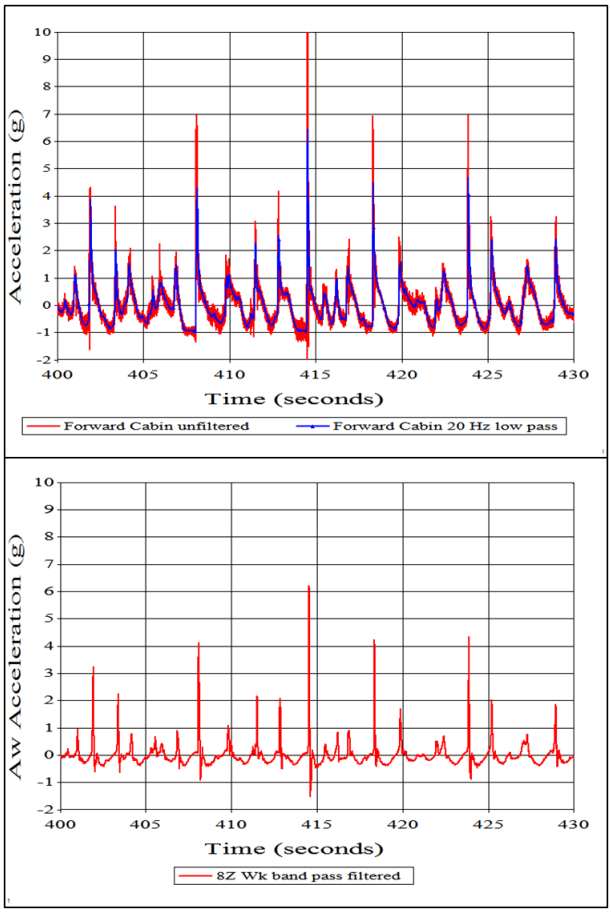

Figure 18. Unfiltered, 20-Hz Low-pass, and Wk Band-pass Filtered Accelerations

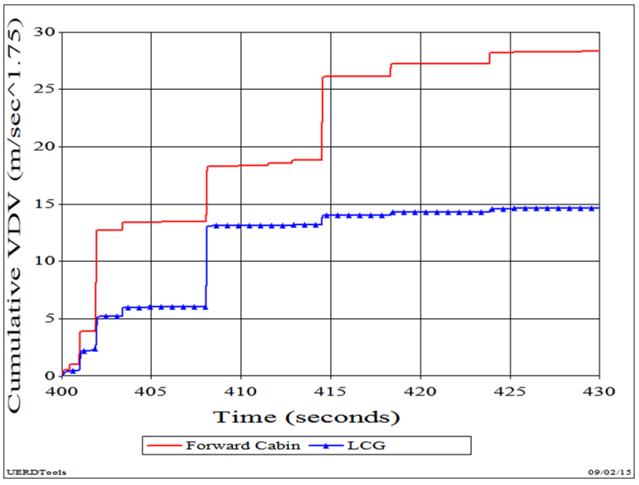

Figure 19. Cumulative VDV Curves for LCG and Forward Cabin

Daily Equivalent Static Compression Dose

The daily equivalent static compression dose (S_{ed}) in megapascals (MPa) is a method for estimating adverse health effects on the spine of a seated human due to whole body vibrations containing multiple shocks [31, 32]. It is computed using equation (5).

$$S_{ed} = \left[\sum_{k=x,y,z} (m_k \, D_{kd})^6 \right]^{1/6} \qquad \text{Equation (5)}$$

where:

$m_x = 0.015$ MPa/m/sec^2

$m_y = 0.035$ MPa/m/sec^2

$m_z = 0.032$ MPa/m/sec^2

and

$$D_{kd} = \left(\sum_{j=1}^{n} D_{kj}^6 \frac{t_{dj}}{t_{mj}} \right)^{1/6} \qquad \text{Equation (6)}$$

where:

D_{kd} is the acceleration dose for the total daily exposure

D_{kj} is the acceleration dose for the jth unique exposure period within a day

k is x, y, z axes

t_{dj} is the duration of the daily exposure to condition j

t_{mj} is the period over which D_{kj} was measured

j is the incremented count of unique daily exposure periods

n is the number of daily exposure periods

and

$$D_k = \left[\sum_i A_{ik}^6 \right]^{1/6} \qquad \text{Equation (7)}$$

where:

D_k is the average acceleration dose in the k direction

A_{ik} is the ith peak of the spine response acceleration $a_{ik}(t)$ in the k axis

The vertical Sed8 value is 0.91 MPa for the forward cabin 30-second segment shown in the upper plot of Figure 18. The Sed8 value for the 30-second LCG acceleration is 0.54 MPa. For the entire 10-minute trial the Sed8 value for the forward cabin location is 12.22 MPa and 7.36 MPa for the LCG.

Rules for computing the spine response acceleration A_i for all three axes and a method for accounting for spine tissue strength and bone density related to age of the seat occupant are provided in ISO 2631 Part 5. Guidance for estimating a low probability and a high probability of adverse effects on the spine are also provided [31].

CONCLUSIONS AND RECOMMENDATIONS

This report is a guide for measuring and analyzing acceleration data recorded during trials of full-scale high speed craft. Minimum requirements for instrumentation systems are summarized, and standardized data processing methods are presented to foster commonality and comparability between different organizations. Examples of recorded data are shown to illustrate data processing and data analysis methods, and numerous approaches to comparing and evaluating data sets are summarized. While the primary focus is on recorded accelerations, the data acquisition, processing, and comparison methods are also applicable to measured pitch, roll, and yaw motions.

In this report both statistical and deterministic approaches for analyzing acceleration data are presented. The statistical methods provide knowledge about acceleration amplitude variation over time in random seaways. The deterministic methods provide knowledge about the physical characteristics of a single impact that can be used in engineering design and laboratory testing applications. When used together the deterministic and statistical analysis approaches provide more knowledge for addressing a broader range of design and comparative analysis investigations than if only one analysis approach is used. It is therefore recommended that all data analysts use both deterministic and statistical analysis approaches.

Successfully data analysis, both deterministic and statistical, relies solely on the quality of the recorded data. It is therefore recommended that close attention be paid to measurement system powering, sensor mounting, signal conditioning (including anti-aliasing filtering), and data recording (including sampling rate).

The example acceleration data shown in this report illustrates the superposition of shock induced rigid body accelerations, shock induced transient structural vibrations, and ambient vibrations (i.e., somewhat steady-state) caused to propulsion machinery and hull-water interactions. The process of analyzing measured accelerations therefore begins with decomposing the measured signal into its fundamental parts, so that each can be characterized and understood. Response mode decomposition is achieved by using a low-pass filter to estimate the rigid body accelerations and a high-pass filter to estimate vibration accelerations. Only after this separation occurs can analyses proceed with studying the effects of vibration accelerations and the effects of rigid body shock accelerations on hull structure, equipment or people.

When studying the effects of wave impacts (i.e., the shock load component) on hull structure, equipment, and people, it is recommended that unfiltered acceleration data containing transient and quasi-steady-state vibration accelerations not be referred to as G-load. Shock loads and the transmission of shock forces throughout a craft are best evaluated by studying rigid body accelerations. The rigid body accelerations are used as a measure of wave impact shock load in units of “g”.

REFERENCES

1. Jasper, N. H., *Dynamic Loading of a Motor Torpedo Boat (YP 110) During High Speed Operation in Rough Water*, David Taylor Model Basin Report C-175, September 1949.
2. DuCane, Peter, *The Planing Performance, Pressures, and Stresses in a High-Speed Launch*, Presented in London at a Meeting of The Institution of Naval Architects,7 June 1956.
3. Fridsma, Gerard, *A Systematic Study of the Rough Water Performance of Planing Boats – (Irregular Waves) – Part II*, Research Report 1495, Davidson Laboratory, Stephens Institute of Technology, Hoboken, N.J., USA, March 1971.
4. Blount, D., Hankley, D., *Full Scale Trials and Analysis of High Performance Planing Craft Data*, Society of Naval and Marine Engineers Number 8, November 1976.
5. Savitsky, Daniel, Koelbel, Joseph G., *Seakeeping Considerations in Design and Operation of Hard Chine Planing Hulls*, Prepared for Combatant Craft Engineering Department, Naval Ship Engineering Center, Norfolk, Virginia, 17 May 1978.
6. Riley, M., Coats, T., Haupt, K., Jacobson, D., *The Characterization of Individual Wave Slam Acceleration Responses for High-Speed Craft*, Proceedings of the American Towing Tank Conference, Annapolis, Maryland, August 2010.
7. ISO-2631-1, *Mechanical vibration and shock – Evaluation of human exposure to whole body vibration – Part 1: General requirements*, International Organization for Standardization, ISO 2631-1:1997(E).Geneva, Switzerland, July 1997.
8. Stanley, William D., Dougherty, Gary R., and Dougherty, Ray, *Digital Signal Processing*, Prentice-Hall, 1984.
9. Strum, Robert D., and Kirk, Donald E., *Discrete Systems and Digital Signal Processing*, Addison-Wesley, 1989.
10. Smith, Strether. *Digital Data Acquisition and Analysis*, A short course presented at Sensors Expo Chicago, June 9, 2008.
11. Judd, Bob, *Everything You Ever Wanted to Know about Data Acquisition, Parts One and Two*, United Electronics Industries, 2008.
12. Meyers, Robert, Smith, Strether, Wilson, Jon, *Applied Measurements and Digital Data*, Course No. 166-199, Technology Training, Inc., 16-20 November 2009.
13. Zseleczky, John, *Behind the Scenes of Peak Acceleration Measurements*, The Third Chesapeake Powerboat Symposium, Annapolis, Maryland, USA, 14-15 June 2012.
14. Coats, Dr. Timothy, *Shock Mitigation – A Familiar Topic in High-Speed Planing Boat Design*, Proceedings of the 74th Shock and Vibration Symposium, San Diego CA, 27-31 October, 2003.

15. Harris, Cecil M., editor-in-chief, *Shock and Vibration Handbook*, Fourth Edition, McGraw-Hill Companies, Inc., New York, New York, 1995.

16. Mantz, Paul A., Costanzo, Fredrick A., *An Overview of UERDTools Capabilities: A Multi-Purpose Data Analysis Package*, Proceedings of the IMAC-XXVII Conference and Exposition on Structural Dynamics, Society of Experimental Mechanics, Inc., 9-12 February 2009, Orlando, Florida, 2009.

17. Riley, Michael R., Coats, Timothy W., Murphy, Heidi P, *Acceleration Response Mode Decomposition for Quantifying Wave Impact Load in High-Speed planing Craft*, The Society of Naval Architects and Marine Engineers, The Fourth Chesapeake Powerboat Symposium, 23-24 June 2014, Annapolis, Maryland, USA.

18. Riley, Michael R., Coats, Timothy W., *The Simulation of Wave Slam Impulses to Evaluate Shock Mitigation Seats for High-Speed Planing Craft*, Naval Surface Warfare Center Carderock Division Report NSWCCD-80-TR-2013/16, May 2013.

19. Riley, Michael R., Haupt, Kelly D., Jacobson, Donald R., *A Generalized Approach and Interim Criteria for Computing $A_{1/N}$ Accelerations Using Full-Scale High-Speed Craft Trials Data*, Naval Surface Warfare Center Carderock Division Report NSWCCD-TM-23-2010/13, April 2010.

20. Murphy, Heidi P., Planchak, Christopher J., *Description of the Rough-Water Dataset Captured On a Shallow-Vee Hull*, Naval Surface Warfare Center Carderock Division Report NSWCCD-80-TR-2015/028, May 2015.

21. Savitsky, Daniel and Brown, P.W. (October 1976). *Procedures for Hydrodynamic Evaluation of Planing Hulls in Smooth and Rough Water*, *Marine Technology*, Volume 13, No. 4.

22. Munk, W. H. (December 1944). *Proposed Uniform Procedure for Observing Waves and Interpreting Instrument Records*, Scripts Institute of Oceanography Wave Report 26.

23. Dobbins, T., Myers, S., Withey, W., Dyson, R., Gunston, T. and King, S., *High Speed Craft Motion Analysis – Impact Count Index (ICI)*, Conference Proceedings; The 43rd United Kingdom Conference on Human Responses to Vibration, Leicester, pp 37-43, 2008.

24. Riley, Michael R., Haupt, Kelly D., Ganey, Dr. H. Neil, *Ride Severity Profile for Evaluating Craft Motions*, Naval Surface Warfare Center Carderock Division Report NSWCCD-80-TR-2015/002, May 2015.

25. Riley, Michael R., Coats, Timothy, Dr., Haupt, Kelly, Jacobson, Donald, *Ride Severity Index: A Simplified Approach for Comparing Peak Acceleration Responses of High-Speed Craft*, The Society of Naval Architects and Marine Engineers, Transactions, Volume 121, pp. 701 – 711, 2013.

26. Riley, Michael R., Haupt, Kelly D., Jacobson, Donald R., *A Deterministic Approach for Characterizing Wave Impact Response Motions of a High-Speed Planing Craft*, Naval Surface Warfare Center Carderock Division Report NSWCCD-23-TM-2012/05, January 2012.

27. Riley, M. R., Coats, T.W., *Development of a Method for Computing Wave Impact Equivalent Static Accelerations for Use in Planing Craft Hull Design*, The Society of Naval Architects

and Marine Engineers, The Third Chesapeake Powerboat Symposium, Annapolis, Maryland, USA, June 2012.

28. Riley, Michael R., Coats, Timothy W., *The Use of Impact Velocity And Peak Acceleration to Quantify Wave Impact Severity For High-Speed Planing Craft*, Naval Surface Warfare Center Carderock Division Report NSWCCD-80-TR-2014/023, Jun 2014.
29. Riley, Michael R., Haupt, Kelly D., Murphy, Heidi, *Test Specification Guide for Electrical and Electronic Equipment to Withstand Wave impacts in Planing Craft*, Naval Surface Warfare Center Carderock Division Report NSWCCD-23-TM-2012/03 Revision A, January 2012.
30. Riley, Michael R., Coats, Timothy W., *Quantifying Mitigation Characteristics of Shock Isolation Seats in a Wave Impact Environment*, Naval Surface Warfare Center Carderock Division Report NSWCCD-80-TR-2015/001, January 2015.
31. ISO-2631-5, *Mechanical vibration and shock – Evaluation of human exposure to whole body vibration – Part 5: Method for Evaluation of Vibration Containing Multiple Shocks*, International Organization for Standardization, ISO 2631-5:2004(E),Geneva, Switzerland, 2004.
32. Petersen, Dr. Ron, Pierce, Eric, Price, Brian, Bass, Dr. Cameron, *Shock Mitigation for the Human on High Speed Craft: Development of an Injury Impact Design Rule*, paper presented at the RTO AVT Symposium on Habitability of Combat and Transport Vehicles: Noise, Vibration and Motion, Prague, Czech Republic, 4 – 7 October 2004.

APPENDIX A. WAVE IMPACT DETERMINISM

Historical Perspective

The earliest data analysis methods for high-speed craft were developed for studies of human ride comfort in high-speed craft. Researchers typically applied vibration signal analysis methods developed originally in the airline and automobile industries [A1]. This led to the practice of using craft acceleration data to compute the root-mean-square (RMS) acceleration value of an entire acceleration signal to quantify ride severity. Subsequent researchers used the root-mean-quad acceleration (RMQ, 4^{th} power root mean) as a measure of severity in an attempt to emphasize the effects of all the acceleration spikes caused by impacts [A2]. Many, but not all, naval architects used averages of the highest peak accelerations to quantify the severity of a run, including the average of the highest 1 percent referred to as $A_{1/100}$, the average of the highest 10 percent denoted $A_{1/10}$, and the average of the highest 33.3 percent denoted $A_{1/3}$.

The characteristics of transient vibration motions are very different from the physical characteristics of craft motions caused by wave impacts [A3, A4]. The applied forces, participating masses, momentum transfers, and resulting heave displacements due to wave impacts are sufficiently different from transient vibrations to suggest each that impact be analyzed and quantified using different mathematical tools. While numerous historical references have made similar statements, the application of different computational techniques for wave impact investigations has only become practical during the past decade.

Earlier researchers applied the mathematical tools that were practical for computational hardware at the time. Now the use of modern hardware and data analysis software enables the next step beyond statistical averaging of entire acceleration signals. The availability of numerical computation and visualization codes such as MATLAB® and UERDTools [A5] enables a new approach to acceleration data analysis referred to as wave impact determinism. Wave impact determinism is simply the analysis of wave impacts one-at-a-time [A6]. It compliments results of statistical analyses by providing additional information related to the cause and effect physical relationships in individual wave impacts (i.e., inputs and responses).

One Wave Impact

A vertical acceleration time history for one wave impact is shown in the upper plot in Figure A1. The figure also shows the velocity and absolute displacement curves obtained by integration. Understanding the physical sequence of events for one wave impact is useful because it helps to visualize and distinguish between the wave impact period and non-impact periods in the acceleration plot. For example, at time A, the -0.9 g vertical acceleration indicates a condition very close to free fall. The relatively constant -0.9 g from time A to time B and the linear decrease in velocity suggests that the craft is rotating downward with the stern in the water. The drop in height from time A to B is most likely a combination of heave and pitch. At time B, the craft impacts the incident wave, the velocity is at a minimum, the negative slope changes rapidly to a positive slope, and the force of the wave impact produces a sharp rise in acceleration. From time B to time C, the craft continues to move down in the water, the velocity

approaches zero, and the acceleration decreases rapidly. At time C the downward displacement of the craft reaches a maximum, the instantaneous velocity is zero, and the impact event is complete. From time C to D forces due to buoyancy, hydrodynamic lift, and components of thrust and drag combine to produce a net positive acceleration. From time D to E, gravity begins to overcome the combined forces of buoyancy, hydrodynamic lift, and components of thrust and drag as another wave encounter sequence begins.

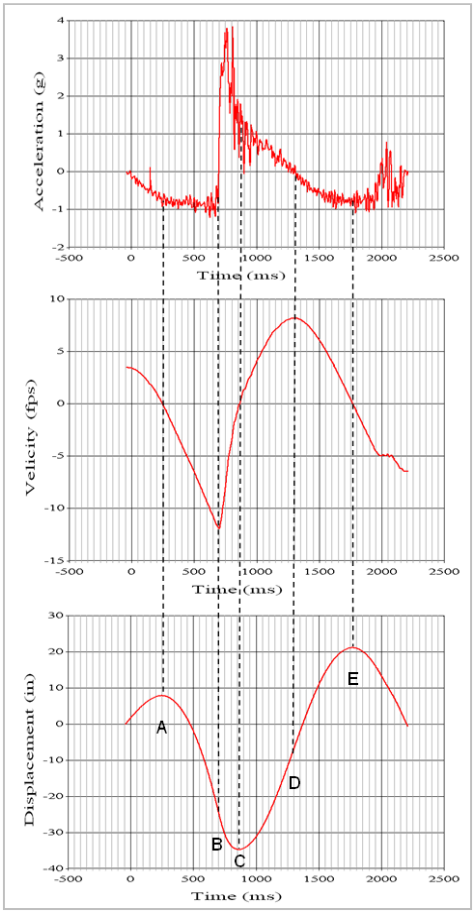

Figure A1. Wave Impact Sequence of Events

The period of time in Figure A1 from point B to point C is the wave impact period. It is this period of time from B to C that will be important for understanding and evaluating the effects of individual wave impacts.

Appendix A REFERENCES

A1. Stark, D.R., *Ride Quality Characterization and Evaluation in the Low Frequency Regime with Applications to Marine Vehicles*, Human Factors in Transport Research Volume 2 User Factors; Comfort, The Environment and Behavior, Academic Press, London, UK, 1980.

A2. Boileau, P.E., Turcot, D., Scory, H., *Evaluation of Whole-Body Vibration Exposure Using a Fourth Power Method and Comparison with ISO 2631*, Journal of Sound and Vibration, Volume 129(1), pp. 143 – 154, 1989.

A3. Gollwitzer, Richard M., Peterson, Ronald S., *Repeated Water Entry Shocks on High-Speed Boats*, Dahlgren Division Naval Surface Warfare Center, Panama City Report CSS/TR-96/27, September 1995.

A4. Coats, Dr. Timothy, *Shock Mitigation – A Familiar Topic in High-Speed Planing Boat Design*, Proceedings of the 74th Shock and Vibration Symposium, San Diego CA, 27-31 October, 2003.

A5. Mantz, Paul A., Costanzo, Fredrick A., *An Overview of UERDTools Capabilities: A Multi-Purpose Data Analysis Package*, Proceedings of the IMAC-XXVII Conference and Exposition on Structural Dynamics, Society of Experimental Mechanics, Inc., 9-12 February 2009, Orlando, Florida, 2009.

A6. Riley, M., Coats, T., Haupt, K., Jacobson, D., *The Characterization of Individual Wave Slam Acceleration Responses for High-Speed Craft*, Proceedings of the American Towing Tank Conference, Annapolis, Maryland, August 2010.

THIS PAGE INTENTIONALLY LEFT BLANK

APPENDIX B. SHOCK RESPONSE SPECTRUM

Mathematical Model

The shock response spectrum (SRS) is a universal mathematical tool used to quantify and compare the severity of different shock motions [B1 – B9]. Example applications include comparing field shock test data (e.g., single severe wave impact) to laboratory test machine data to ensure laboratory tests simulate the severity of actual field conditions, or comparing field shock test data to draft shock design levels to ensure shock design criteria conservatively envelope actual field conditions. SRS are also used for evaluating how systematic changes in test parameters affect shock response severity, and for comparing how rigid seats and shock isolation seats respond to vertical shock inputs [B10 - B12]. It has also been used to specify the severity of laboratory machine tests for demonstrating that equipment can survive single severe wave impacts. The SRS is a versatile tool with applications in structural strength, equipment ruggedness, ejection seat performance, and measuring ride comfort in land vehicles and high-speed boats [B3].

Before introducing the shock response spectrum, the following paragraphs present an example calculation to illustrate how a mathematical model of a single-degree-of-freedom system is used to evaluate and compare the severity of two different shock motions that have the same peak acceleration, but different durations, different changes in velocity, and different average values of jerk.

Figure B1 shows a model of a single-degree-of-freedom (SDOF) system. The system has a base attached to a mass (m) by a spring (with stiffness k) and a damper (with damping coefficient c). For a prescribed shock input motion y (t) at the base of the system the resulting response of the mass (m) is x (t). The relative displacement z (t) between the base and the mass is x (t) minus y (t). The equation of motion of the system (i.e., equation B1) is obtained by summing the inertial force of the mass and the forces within the spring and damper [B2].

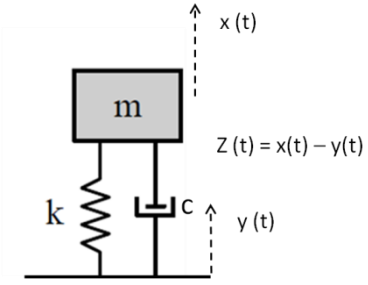

Figure B1. Single-degree-of-freedom Mathematical Model

$$m\,\ddot{x}(t) = k\,z(t) + c\,\dot{z}(t) \qquad \text{Equation (B1)}$$

The dot and double dot represent the first and second derivatives, respectively. With appropriate substitutions, equation B1 can be rewritten as equation B2 and solved for the relative displacement z (t). Mathematical solutions to equation (B2) for different pulse shapes are presented in reference B3.

$$m\ddot{z} + 2\xi\omega\dot{z} + \omega^2 z = -\ddot{y} \qquad \text{Equation (B2)}$$

The damping factor, or damping ratio, is given by equation B3.

$$\xi = \frac{\mathrm{c}}{2\,\mathrm{m}\,\omega} \qquad \text{Equation (B3)}$$

The natural frequency (f) in Hertz (Hz) of the SDOF system is given by equation B4.

$$\mathrm{f} = \frac{\omega}{2\pi} = \left(\frac{1}{2\pi}\right)\sqrt{\frac{k}{m}} \ \ \mathrm{Hz} \qquad \text{Equation (B4)}$$

The maximum predicted acceleration response of the SDOF mass (m) is a parameter for comparing shock severity because it is proportional to the maximum inertial force (i.e., shock force) acting on the mass as a result of the shock input. Likewise, the maximum predicted relative displacement across the SDOF spring is a useful measure because it is proportional to the maximum strain in the spring. Both maximum values (i.e., peak acceleration response and maximum relative displacement) are a measure of the severity of the shock input (in terms of SDOF model response). When two different shock pulses are being compared, the one that results in the larger maximum acceleration and larger relative displacement in the SDOF model is the more severe shock pulse. This is illustrated further in the following paragraphs.

The left plot in Figure B2 shows two hypothetical shock pulses with the same 8-g peak acceleration arbitrarily denoted shock input A and B. Shock pulse B has the longer duration (175 milliseconds (msec) versus 100 msec). For the purpose of the mathematical comparison a SDOF mathematical model with a 9% damping ratio and a natural frequency of 13.5 Hz is arbitrarily selected to evaluate severity in the response domain. The plot on the right in Figure B2 shows the predicted absolute acceleration responses of the mass (m) caused by shock pulse A and shock pulse B. The peak acceleration response for pulse A is predicted to be 11.39 g and the peak response for pulse B is 8.46 g. These values along with the predicted maximum relative displacements for the SDOF system are listed in Table B1. The predicted maximum relative displacement for pulse A is 0.015 millimeters and for pulse B it is 0.011 millimeters. These results in the response domain indicate that pulse A is predicted to result in a larger peak acceleration response and a larger maximum relative displacement, thus pulse A is more severe than shock pulse B for a 13.5-Hz SDOF system.

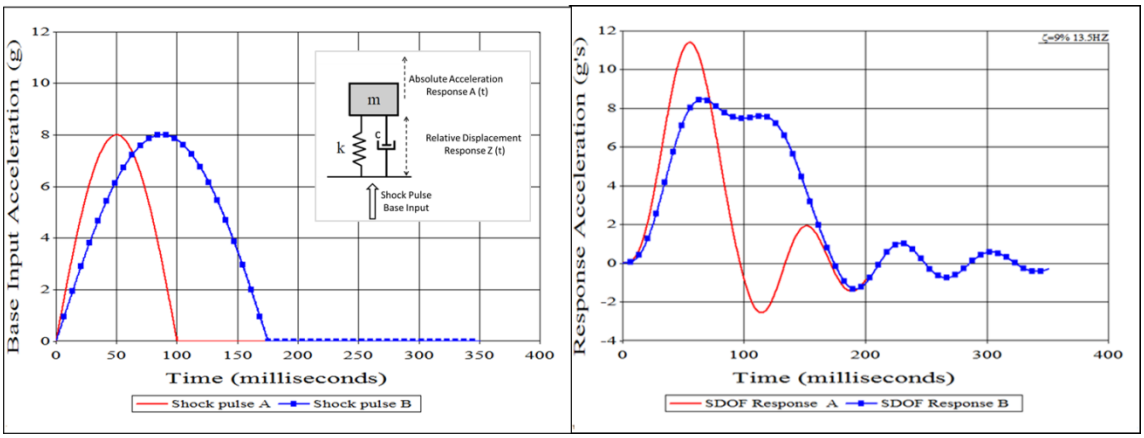

Figure B2. 13.5-Hz SDOF System Input and Predicted Response Accelerations

In this example the 13.5-Hz SDOF system was chosen arbitrarily to illustrate the comparison. When many other calculations are made for other values of SDOF system natural frequency, the plot of the maximum response (either peak acceleration response or maximum relative displacement) for a given shock input versus system natural frequency is referred to as a shock response spectrum. It is a plot of SDOF system maximum shock response versus SDOF model natural frequency. The following examples illustrate the shock response spectrum concept.

Table B1. 13.5-Hz SDOF System Maximum Responses

Shock Pulse Input	13.5 Hz System Response			
	Response A $_{MAX}$		Response Z $_{MAX}$	
	m/sec^2	g	mm	inch
A	111.736	11.390	0.015	0.606
B	82.993	8.460	0.011	0.449

The acceleration plots in Figure B3 show predicted response motions (i.e., acceleration versus time) for a 30-Hz SDOF system (red circles) and a 5-Hz SDOF system (blue triangles). The shock input motion for each prediction was assumed to be a half-sine acceleration pulse with a peak of 10 g and 50-millisecond duration (black curve). The maximum response acceleration predicted for the 30-Hz system is 13.6 g. The maximum response predicted for the 5-Hz system is 8.2 g. Thus it is observed that the maximum response (i.e., peak acceleration in this example) of the SDOF system is a function of the natural frequency (f) of the SDOF model.

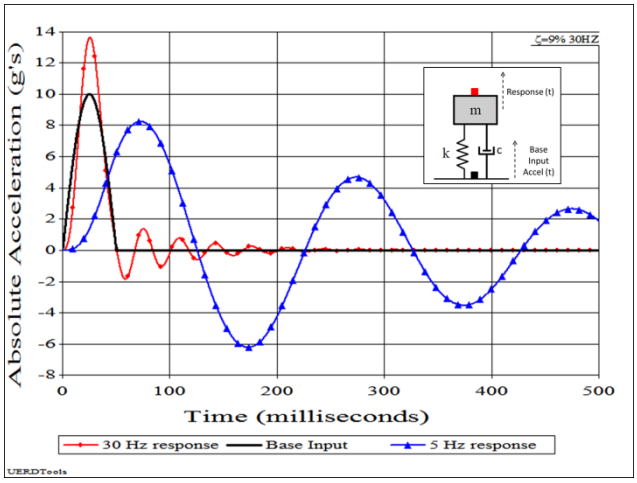

Figure B3. SDOF Model with Sample Base Input and Predicted Responses

Figure B4 is a plot of the maximum acceleration response of the SDOF model for model natural frequencies from 4 Hz to 80 Hz for the 10 g – 50 msec base input pulse. It is called an acceleration shock response spectrum (ASRS). The symbols in the figure identify the two predicted peak response values shown in Figure B3 (i.e., 13.6 g for 30 Hz and 8.2 g for 5 Hz).

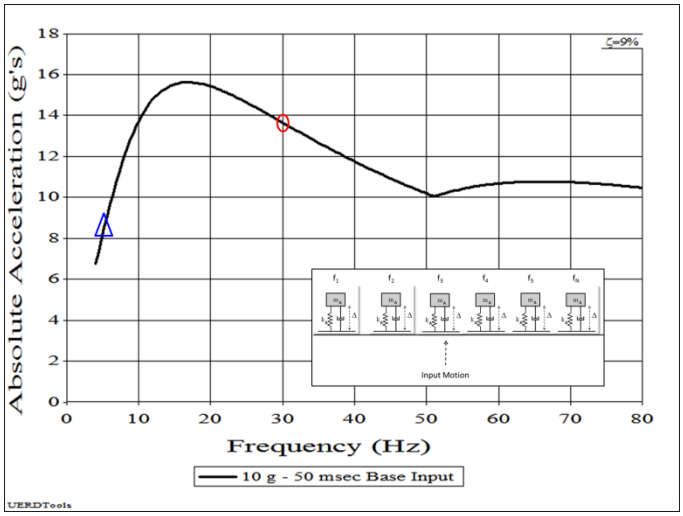

Figure B4. Acceleration SRS for 10g-50 msec Base Input

The maximum response of the SDOF system can also be plotted as a function of the maximum compressive relative displacement (Z_{MAX}) across the SDOF model's spring. Figure B5 shows a plot of the maximum compressive relative displacement caused by the 10 g-50 msec base input acceleration (half sine) as a function of model natural frequency. It is called a relative displacement SRS (DSRS).

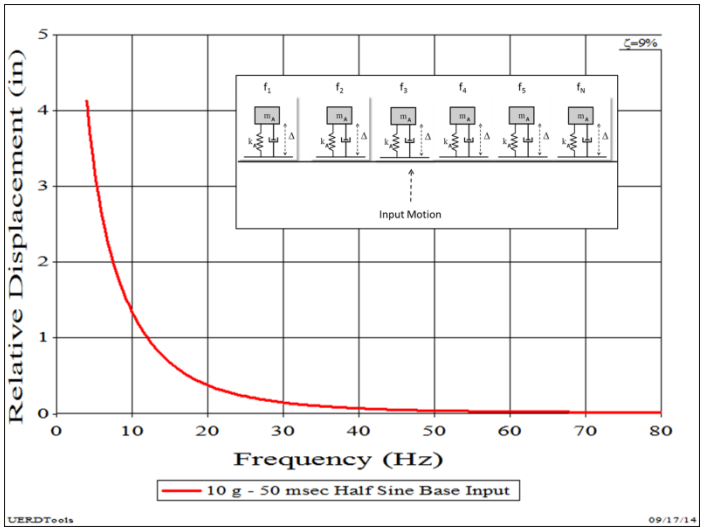

Figure B5. Maximum Relative Displacement SRS

Dynamic Response Index

The maximum compressive relative displacement from an SRS computed for a SDOF model with a natural frequency of 8.4 Hz and damping ratio of 0.22 is often used for evaluating the effects of single impact loads on seated humans. For example, it is used in an international test standard for evaluating the safety of passengers in lifeboats that are dropped vertically from large ships during emergencies [B10]. It is also used in a specification for aeronautical seats to evaluate pilot safety when exposed to a vertical impulsive load during simulated ejection in aircraft and escape capsules [B11], and for evaluating shock isolation seat mitigation for marine craft [B12].

The maximum compressive relative displacement (Z_{MAX}) from an SRS computed for a natural frequency of 8.4 Hz and damping ratio of 0.22 is proportional to a term referred to as the Dynamic Response Index (DRI) given by equation B5 [B11, B13].

$$DRI = \frac{\omega_n^2 Z_{MAX}}{g} \qquad \text{Equation (B5)}$$

where:

$\omega_n = 52.9$ rad/sec (i.e., 8.4 Hz from equation B4)

g = acceleration due to gravity

Appendix B REFERENCES

B1. ISO-18431-4: 2007, *Mechanical vibration and shock – Signal processing – Part 4: Shock response spectrum analysis*, International Organization for Standardization, Geneva, Switzerland, 2007.

B2. ANSI/ASA S2.62-2009, *Shock Test Requirements for Equipment in a Rugged Shock Environment*, American National Standards Institute, Acoustical Society of America, Melville, N.Y., 9 June 2009.

B3. Harris, Cecil M., editor-in-chief, *Shock and Vibration Handbook*, Fourth Edition, McGraw-Hill Companies, Inc., New York, New York, 1995.

B4. Department of Defense Test Method Standard, *Environmental Engineering Considerations and Laboratory Tests*, Military Standard, MIL-S-810G, Method 516.6, Shock, 31 October 2008.

B5. ASTM D5487:2008, *Standard Test Method for Simulated Drop of Loaded Containers by Shock Machines*, American Society of Testing and Materials, West Conshohocken, Pennsylvania, April 2008.

B6. Department of Defense Test Method Standard, *Electronic and Electrical Component Parts*, Military Standard, MIL-STD-202G, Method 213B, Shock, 16 April 1973.

B7. North Atlantic Treaty Organization Standard Agreement NATO STANAG 4370, Method 417, *SRS Shock*, 31 May 1994.

B8. Alexander, J. Edward, *The Shock Response Spectrum – A Primer*, Society of Experimental Mechanics Inc., Proceedings of the IMAC XXVII, Orlando, Florida, USA, 9 – 12 February 2009.

B9. Gaberson, Howard A., *Shock Severity Estimation*, Sound and Vibration Magazine, Volume 46 Number 1, January 2012.

B10. *Testing and Evaluation of Life-Saving Appliances*, Maritime Safety Committee Resolution MSC.81(70), Life-Saving Appliances, 2003 Edition, International Maritime Organization, 2003.

B11. Wright, Nathan, Pellettiere, Joseph A., Fleming, Scott M., Smith, Susan D., Jurcsisn, Jennifer G., *Seat Interfaces for Aircrew Performance and Safety*, Air Force Research Laboratory Report AFRL-RH-WP-TR-2010-0083, January 2010.

B12. Riley, Michael R., Haupt, Kelly D., Ganey, Dr. H. C. Neil, Coats, Dr. Timothy W., *Laboratory Test Requirements for Marine Shock Isolation Seats*, Naval Surface Warfare Center Carderock Division Report NSWCCD-TR-80-2015/010, May 2015.

B13. Payne, Peter R., *On Quantizing Ride Comfort and Allowable Acceleration*, Payne Incorporated - David Taylor Naval Ship Research and Development Center Paper 196-6, Bethesda, Maryland, July 1976.

THIS PAGE INTENTIONALLY LEFT BLANK

APPENDIX C. SELECTION OF LOW-PASS CUTOFF FREQUENCY

Cutoff Frequency

Figure C1 shows the amplitude functions for 2-pole and 4-pole Butterworth low-pass filters. The amplitude reduction at the cutoff frequency is equal to $1/\sqrt{2}$ (i.e., 0.707) [C1]. The cutoff frequency for each calculated curve in the figure was set at 10 Hz. The amplitude scale is set to 1.0 at 0 Hz (i.e., direct current) to illustrate the attenuation provided by each filter. The frequency scale represents different frequencies in the acceleration signal. It is important to note that the 10 Hz low-pass filter does not pass all frequency content below 10 Hz nor does it remove all frequency content above the cutoff. This is characteristic of all low-pass filters. For example, in Figure C1 the 8 Hz content in an acceleration signal would be passed with reduction factors of 0.84 for the 2-pole filter (i.e., 16% attenuation) and 0.92 for the 4-pole filter (i.e., 8% attenuation). Likewise, frequencies above the cutoff frequency are not completely removed. The 2-pole filter has reduction factors at 20 Hz and 30 Hz of 0.24 and 0.062, respectively (i.e., 76% and 93.8% attenuation). For the 4-pole filter the reduction factors for 20 Hz and 30 Hz are 0.11 and 0.012, respectively (i.e., 89% and 98.8% attenuation). Experience has shown that a 4-pole Butterworth low-pass filter is effective for estimating rigid body content by attenuating vibration content above approximately 20 Hz.

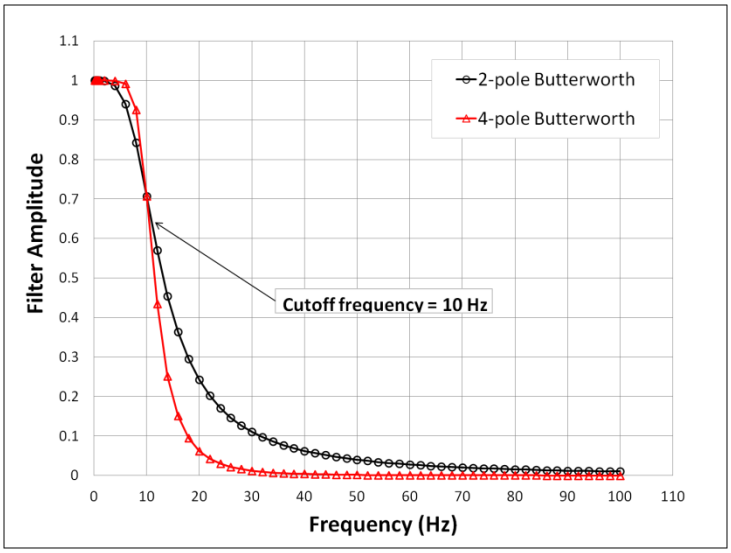

Figure C1. Filter Amplitude Functions

Low-pass Filtering

The tutorial documents that describe the StandardG computational process suggest that a 10 Hz low-pass filter be used to extract peak rigid body vertical accelerations (i.e., heave accelerations) caused by wave impacts *unless some other cutoff value is indicated by frequency analysis (i.e., FFT analysis)* [C2]. This is illustrated in Figure C2 that shows the vertical acceleration recorded during two wave impacts in an aluminum 11-meter rigid-hull inflatable boat (RIB). The red curve is the unfiltered acceleration and the green curve is the 10 Hz low-pass filtered data. The 10 Hz cutoff value was confirmed by looking at the Fast Fourier Transform (FFT) plot of the entire acceleration record shown in Figure C3.

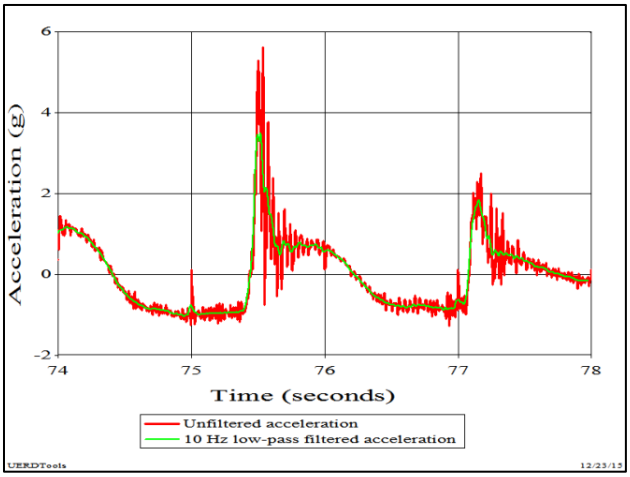

Figure C2. Unfiltered and Low-pass Filtered Acceleration Data

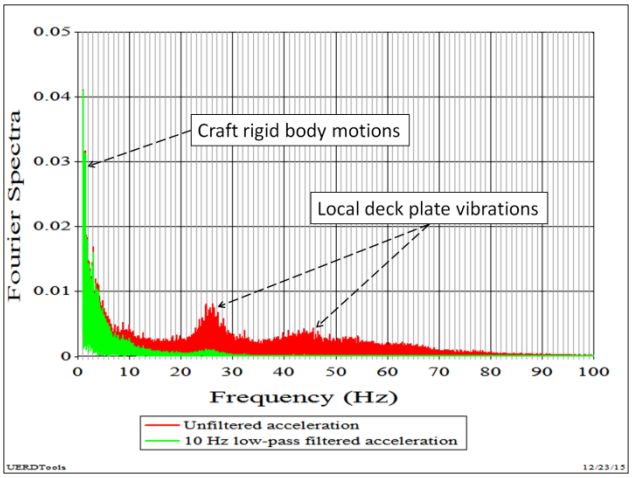

Figure C3. Unfiltered and Low-pass Filtered FFT Plots

The Fourier transform converts the original acceleration signal into a summation of sinusoidal functions [C3]. The FFT plots in Figure C3 show the relative amplitude of the different frequency sinusoids used to construct the original acceleration plot shown in Figure C2.

The deck vibration content is shown by the humps in the red curve (i.e., the FFT for the unfiltered data) at approximately 25 Hz and 40 to 70 Hz. The FFT of the 10 Hz low-pass filtered acceleration data is the green curve. It clearly shows how the vibration content from 20 Hz to 70 Hz and higher has been significantly attenuated. The rigid body heave content in each signal is illustrated by the wave encounter frequency (i.e., the spikes below 2 Hz), and the varying wave impact pulse durations from roughly 1.25 Hz to 5 Hz (i.e., half-sine pulses with 0.10 to 0.40 second durations).

In Figure C2 the phase delay caused by the low-pass filter has been removed by shifting the filtered record 0.0254 seconds to the left. The figure illustrates how proper selection of the low-pass cutoff frequency maintains the shape, amplitude, and duration of the acceleration pulse caused by the wave impact. For the impact pulse observed at approximately 75.5 seconds the rate of acceleration application (i.e., the acceleration jerk) is approximately the same for the filtered and unfiltered curves. The peak acceleration of the filtered curve is observed as a rough average of the high frequency oscillations, and the duration of the pulses (approximately 0.195 seconds) are approximately the same.

Cutoff frequencies less than 10 Hz are not typically recommended for high-speed craft data because of the possibility of a reduction in the indicated wave impact velocity (i.e., the area under the acceleration pulse). The following examples illustrate special cases where a cutoff frequency greater than 10 Hz was selected to attenuate vibrations and analyze structural responses in a high-speed craft.

Unique Deck Oscillations

Figure C4 shows an example where a 30 Hz low-pass filter was used to evaluate unique motions of the deck of an 11 meter (m) cabin rib made of composite material. The plot shows a wave impact event that occurred in the time history at approximately 55.1 seconds. The red curve is the unfiltered acceleration recorded in the vertical direction at the base of a shock isolation seat. It shows an acceleration pulse from approximately 55.1 seconds to 55.24 seconds, followed by a negative seat-bottom impact spike at 55.24 seconds, and then low frequency deck oscillations in the 7 Hz to 9 Hz range.

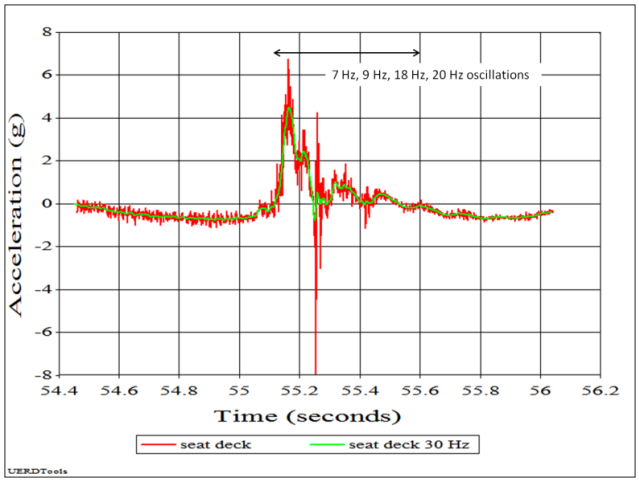

Figure C4. Unique Deck Oscillation Using 30 Hz Low-pass Filter

During the wave impact, before the seat bottom impact, two cycles of deck oscillation are observed with periods that correspond to 18 Hz to 20 Hz. Analysis of other accelerations recorded at several deck and deckhouse locations indicated that the unique oscillations were caused by a composite deck house fore-aft flexural mode with dominant frequencies in the 17 Hz to 24 Hz range. After the seat bottom impact (i.e., at 55.24 seconds) the deck oscillations are observed to damp out with durations that correspond to approximately 7 Hz to 9 Hz. Analysis of other gage location data indicated the oscillations after the seat bottom impact were driven by a roughly 7 Hz to 8 Hz composite hull girder whipping mode. A 30 Hz low-pass filter was selected to analyze and quantify deck motions and shock isolation seat response motions after examination of the Fast Fourier Transform (FFT) plot shown in Figure C5. The selection of the 30 Hz low-pass filter was based on the desire to remove vibration content above approximately 37 Hz and to retain the 7 Hz to 20 Hz deck motions caused by hull girder whipping and deck house flexure. The FFT plot in Figure C5 shows how the 30 Hz low-pass filter attenuates the frequency content above 30 Hz and retains the majority of the 7 Hz to 20 Hz frequency content of interest.

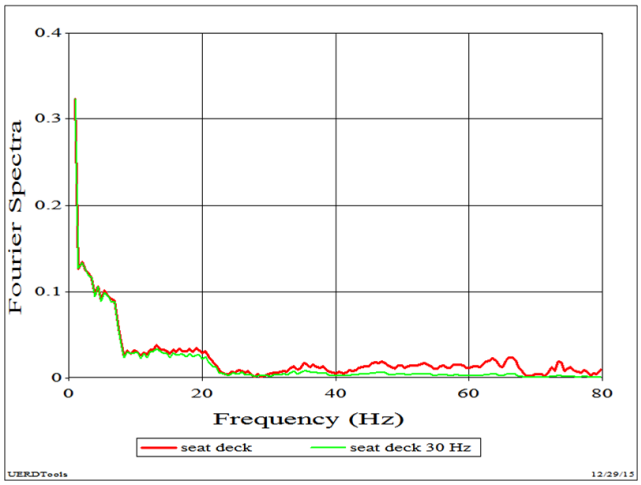

Figure C5. FFTs of Unique Deck Oscillation and 30 Hz Low-pass Filtered Data

Over Filtering

Over-filtering occurs when a cut-off frequency is selected that is too low for the application. This can be detected by comparing the low-pass filtered acceleration data with the original unfiltered data in the time domain. Figure C6 shows an example where a 10 Hz low-pass filter results in over-filtering the acceleration data. The red and green curves are the same unfiltered and 30 Hz low-pass filtered accelerations shown in Figure C4. The dark blue curve is the acceleration time history after it was low-pass filtered using a 10 Hz cutoff frequency. The general characteristics of an over-filtered acceleration pulse, corresponding to the 10 Hz low-pass filtered data, include a reduced rate of acceleration application (i.e., jerk or acceleration slope), a reduced peak acceleration that does not average through the high frequency vibration oscillations, and an increased pulse duration. The light blue curve is for a 5 Hz low-pass filter to further illustrate the effects of over-filtering.

Figure C7 shows the over filtering effects in the frequency domain (i.e., the FFT plot). The red curve is the FFT of the unfiltered acceleration data. The green curve is the FFT of the 30 Hz low-pass filtered data, the dark blue curve is the FFT for the 10 Hz low-pass filtered data, and the light blue curve is the FFT for the 5 Hz low-pass filtered data. The figure clearly shows how the 5 Hz and 10 Hz low-pass filters significantly attenuate the 7 Hz to 20 Hz frequencies of interest.

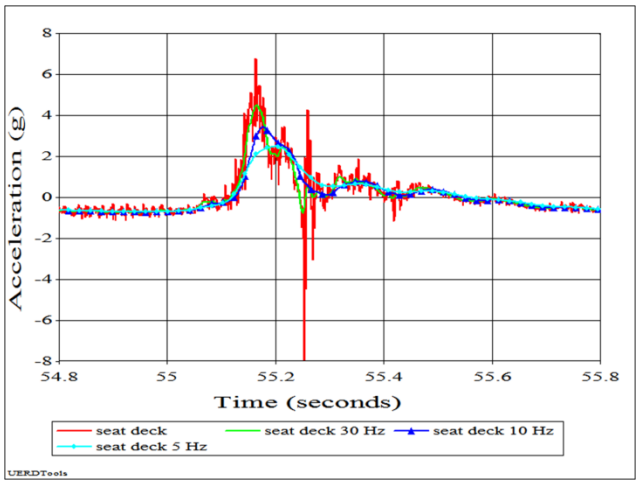

Figure C6. Example of 10 Hz Low-pass Over-Filtered Acceleration Data

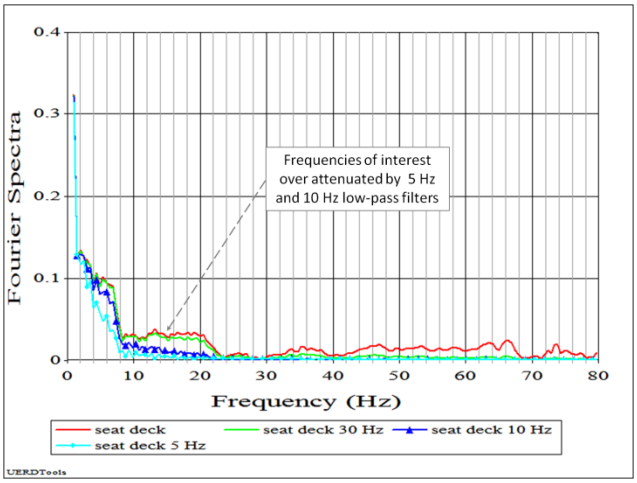

Figure C7. Example 10 Hz Low-pass Over-Filtered FFT Plots

Acceptable Low-pass Filtering

As a general guide, there are four visual observations that can be used to conclude that acceptable low-pass filtering of an acceleration record has been achieved (i.e., no over filtering).

1. The rate of acceleration application (i.e., jerk) of the filtered record is approximately the same as the unfiltered record. See Figures C4 and C6.

2. The peak acceleration of the filtered record is observed to be approximately half-way between the vibration peaks and dips in the record. Depending upon the contiguous structure surrounding the gage position, the vibration signal during the impact (i.e., near the peak acceleration) may not be a symmetric signal with equal peaks and dips. See Figures C4 and C6.

3. The pulse duration of the low-pass filtered acceleration is approximately equal to the duration of the unfiltered acceleration. See Figures C4 and C6.

4. The maximum negative velocity of the filtered record is approximately the same as the maximum negative velocity of the unfiltered record. See Figure C8.

In Figure C8 the velocity curves for the unfiltered data (i.e., red curve) and the 30 Hz low-pass filtered data (i.e., green curve) are almost identical, indicating acceptable low-pass filtering. The changing slopes and changing negative peak amplitudes for the 5 Hz (i.e., light blue) and 10 Hz low-pass filtered data (i.e., dark blue) are indications of over-filtering.

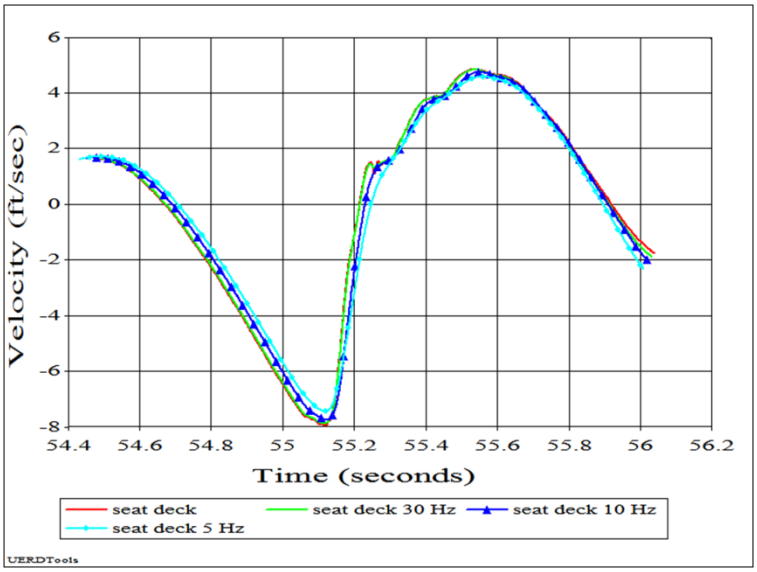

Figure C7. Example of Over Filtered Velocity Plots

Appendix C REFERENCES

C1. Stanley, William D., Dougherty, Gary R., and Dougherty, Ray, *Digital Signal Processing*, Prentice-Hall, 1984.

C2. Riley, Michael, R., Coats, Timothy, W., "A Simplified Approach for Analyzing Accelerations Induced by Wave Impacts in High-Speed Planing Craft", The Society of Naval Architects and Marine Engineers, The Third Chesapeake Powerboat Symposium, Annapolis, MD, 15-16 June 2012.

C3. Webster, John, G., (1999). "The Measurement, Instrumentation, and Sensors Handbook", CRC Press LLC, Boca Raton, FL, USA.

Distribution

	Hard Copies	*Digital Copies*
Naval Sea Systems Command PEO Ships, PMS 325G 1333 Isaac Hull Ave, SE Building 197 Washington Navy Yard, DC 20376 Attn: Christian Rozicer		1
Naval Sea Systems Command TWH Small Boats and Craft 2600 Tarawa Court, Suite 303 Virginia Beach, VA 23459 Attn: Mr. Dean Schleicher		1
Commander Office of Naval Research Sea Platforms and Weapons Division 875 North Randolph Street, Arlington, VA 22203-1995 Attn: Dr. Robert Brizzolara, Code 333		1
Commander Naval Special Warfare Group Four 2220 Schofield Road Virginia Beach, VA 23459 Attn: Sandor Horvath, Code N8		1
United States Naval Academy Hydromechanics Lab 590 Holloway Road Annapolis, MD 21402 Attn: John Zseleczky		1
United States Coast Guard Office of Boat Forces, CG 731 2100 Second Street, SW STOP 356 Washington, DC 20593-7356 Attn: David Shepard		1
United States Coast Guard RDT&E Division 2100 Second Street, SW STOP 7111 Washington, DC 20593-7111 Attn: W. Lew Thomas		1
Defense Technical Information Center 8725 John J. Kingman Road Fort Belvoir, VA 22060-6218		1

NSWC, CARDEROCK DIVISION INTERNAL DISTRIBUTION

Code	Name	*Hard Copies*	*Digital Copies*
661	Rhonda Ingler		1
809	Donna Intolubbe		1
836	Technical Data Repository		1
830X	Dr. Timothy Coats		1
831	Willard Sokol, III		1
832	Scott Petersen		1
833	Kent Beachy		1
833	Dr. Evan Lee		1
835	David Pogorzelski		1
835	Kelly Haupt		1
835	Heidi Murphy		1
835	Brock Aron		1
835	Jason Bautista		1
835	John Barber		1
1033	TIC-SCRIBE		1

NSWC PANAMA CITY

Code	Name	*Hard Copies*	*Digital Copies*
E41	Eric Pierce		1
E23	Brian Price		1
E41	Jeff Blankenship		1


NAVSEA
WARFARE CENTERS
Carderock